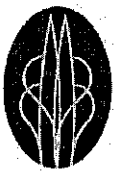

UNIVERSITI
TEKNOLOGI
PETRONAS

Responses of Triangular Tension Leg Platform Subjected to Random Waves

by

Mohd Audi Ashraaf Bin Mohd Zim

Dissertation submitted in partial fulfilment of
the requirements for the
Bachelor of Engineering (Hons)
(Civil Engineering)

JANUARY 2008

Universiti Teknologi PETRONAS
Bandar Seri Iskandar
31750 Tronoh
Perak Darul Ridzuan

CERTIFICATION OF APPROVAL

Responses of Triangular Tension Leg Platform Subjected to Random Waves

by

Mohd Audi Ashraaf Bin Mohd Zim

A project dissertation submitted to the
Civil Engineering Programme
Universiti Teknologi PETRONAS
in partial fulfilment of the requirement for the
BACHELOR OF ENGINEERING (Hons)
(CIVIL ENGINEERING)

Approved by,

(AP Dr. Narayanan Sambu Potty)

UNIVERSITI TEKNOLOGI PETRONAS

TRONOH, PERAK

January 2008

CERTIFICATION OF ORIGINALITY

This is to certify that I am responsible for the work submitted in this project, that the original work is my own except as specified in the references and acknowledgements, and that the original work contained herein have not been undertaken or done by unspecified sources or persons.

MOHD AUDI ASHRAAF BIN MOHD ZIM

ABSTRACT

Tension leg platform (TLP) is suitable for deep water oil and gas exploration. The nonlinear dynamic response analysis of TLP under random sea wave load is necessary for determining the maximum deformations and stresses. Accurate and reliable responses are needed for optimum design and control of the structure. In this project nonlinear dynamic analysis of TLP is carried out in the frequency domain. The time history of random wave is generated based on Pierson-Moskowitz spectrum and acts on the structure in arbitrary direction. The hydrodynamic forces are calculated using the modified Morison's equation according to Airy's linear wave theory. The motion spectrum density of displacements is calculated from linear responses. The focus of the paper is on the comprehensive interpretation of the responses of the structure related to wave excitation and structural characteristics. A case study is investigated and numerical results are discussed.

ACKNOWLEDGEMENT

First of all, I would like to convey my deepest gratitude to my supervisor, AP Dr. Narayanan who continuously supported and guided me from the beginning to the end of my study on this topic. Here, I would also like to express my full appreciation towards AP Dr. Kurian for his generous assistance in conveying his knowledge, experience and understanding towards my project. Not to forget, my colleagues; Gasim, Norhidayah Ngadni, Hannis Sazali and Wong Bak Shiun, Abu Bakr, and Rosni in sharing information throughout many discussions. Also to UTP, especially Civil Engineering Department, for constantly providing me with either formal or informal support throughout the study of this project. The last but not least, thanks to my beloved family and friends who motivated me to achieve this far. Thanks again to all, your kindness and help will always be remembered.

TABLE OF CONTENTS

ABSTRACT iii

ACKNOWLEDGEMENT iv

CHAPTER 1 : INTRODUCTION 1

1.1 Background 1

1.2 Problem Statement 3

1.3 Objectives 4

1.4 Scope of Study 5

CHAPTER 2 : LITERATURE REVIEW 8

2.1 Introduction 8

2.2 Early Studies 8

2.3 Small-Amplitude Wave Theory 10

2.4 Morison's Equation 12

2.5 Pierson-Moskowitz Spectrum 13

2.6 Response Amplitude Operator 15

2.7 Motion-Response Spectrum 16

CHAPTER 3 : METHODOLOGY 18

3.1 Introduction 18

3.2 Identification of Important Parameters 18

3.3 Wave Force Calculation 19

3.4 Wave and Motion Spectrum Development 21

3.5 Parametric Study 22

3.6 Hazards Evaluation 23

CHAPTER 4 : RESULTS AND DISCUSSIONS 25

4.1 Introduction 25

4.2 Random Waves, Wave Forces and TLP Response 25

4.3 Parametric Study 29

CHAPTER 5 : CONCLUSIONS 42

REFERENCES 43

LIST OF FIGURES

Figure 1.1 : Typical TLP Configuration 1

Figure 1.2 : Hutton TLP 2

Figure 1.3 : Location Map of Hutton TLP 2

Figure 1.4 : Definition of rigid body motion modes 6

Figure 1.5 : Details of Triangular Tension Leg Platform 7

Figure 2.1 : Wave spectra of a fully developed sea for different wind speeds according to Moskowitz (1964). 15

Figure 3.1 : Steps for wave force calculation 20

Figure 3.2 : Steps of computing motion RAO 21

Figure 4.1 : Water depth versus wave forces (Hull 1 & 2) 26

Figure 4.2 : Pierson-Moskowitz Spectrum 26

Figure 4.3 : Wave Surface Profile 27

Figure 4.4 : Surge Profile 28

Figure 4.5 : Heave Profile 28

Figure 4.6 : Surge Motion RAO for various significant wave height, H_s 30

Figure 4.7 : Surge Motion Spectrum for various significant wave heights, H_s 30

Figure 4.8 : Heave Motion RAO for various significant wave heights, H_s 31

Figure 4.9 : Heave Motion Spectrum for various significant wave heights, H_s 31

Figure 4.10 : Surge Motion RAO for different water depth 33

Figure 4.11 : Surge Motion Spectrum for different water depth 33

Figure 4.12 : Heave Motion RAO for different water depth 34

Figure 4.13 : Heave Motion Spectrum for different water depth 34

Figure 4.14 : Surge Motion RAO by varying triangular TLP draft 36

Figure 4.15 : Surge Motion Spectrum by varying triangular TLP draft 36

Figure 4.16 : Heave Motion RAO by varying triangular TLP draft 37

Figure 4.17 : Heave Motion Spectrum by varying triangular TLP draft 37

Figure 4.18 : Surge Motion RAO for different initial tether tension 39

Figure 4.19 : Surge Motion Spectrum for different initial tether tension 39

Figure 4.20 : Heave Motion RAO for different initial tether tension 40

Figure 4.21 : Heave Motion Spectrum for different initial tether tension 40

LIST OF TABLES

Table 3.1 : Study of triangular TLP subjected to different significant wave height 22
Table 3.2 : Study of triangular TLP at different water depth 22
Table 3.3 : Study of triangular TLP with different drafts 23
Table 3.4 : Study of triangular TLP with different initial tether tension 23
Table 4.1 : Maximum pitch response subjected to different H_{max} 29
Table 4.2 : Maximum pitch response at different water depth 35
Table 4.3 : Maximum pitch response for different draft 38
Table 4.4 : Maximum pitch response for various initial tether tension 41

LIST OF APPENDICES

Appendix 1 : Wave Force Calculation 44
Appendix 2 : Pierson Moskowitz and Motion Spectra 45
Appendix 3 : Stiffness (Surge, Heave and Pitch) 46
Appendix 4 : Total Mass (Surge, Heave and Pitch) 47

CHAPTER 1
INTRODUCTION

1.1 Background

A Tension Leg Platform (TLP) is a floating platform which is connected to the seabed by vertical tendons or tethers. The tendons are kept under tension by the buoyancy of the platform and this pre-tension is designed to keep the tendons under tension under all circumstances, even in large waves with high crests and deep troughs. The stiff connection of the platform with the seabed reduces the vertical motions to a minimum. A configuration of a typical TLP is shown in Figure 1.1.

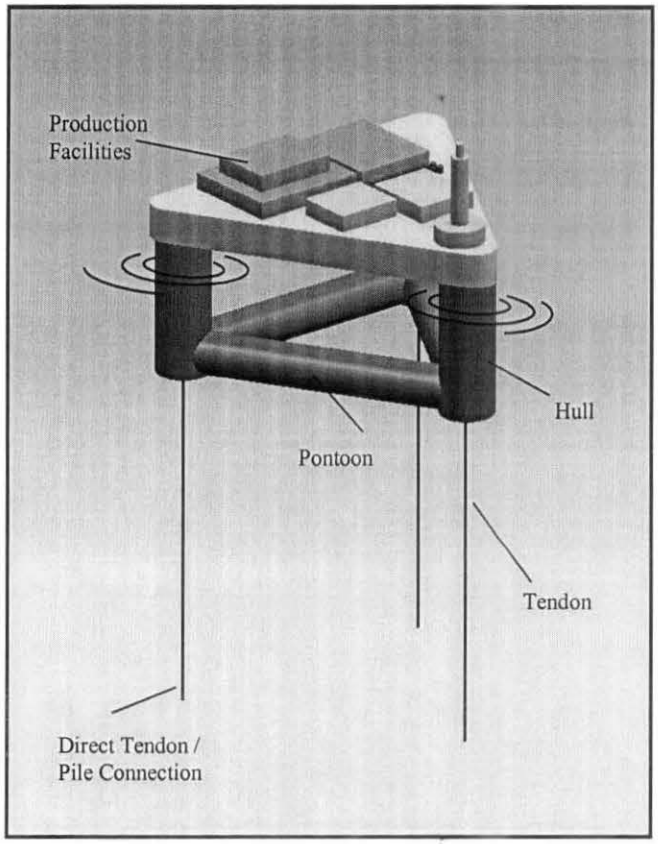

Figure 1.1 : Typical TLP Configuration

Application of Archimedes Principle makes the structure to float in the water. Volume of water displaced by the TLP hulls and pontoons are basically contributing to the excess of buoyancy over the weight of the structure. Part of the hull which is submerged under the water is called draft.

Tendon is made up of strong steel wire rope or cable with certain specified stiffness produced by the manufacturers. The main function of mooring system is to keep the TLP in-place whilst giving small allowance to move in horizontal direction.

The first Tension Leg Platform was built for Conoco's Hutton field in the North Sea in the early 1980s (Figure 1.2 and 1.3). The hull was built in the dry-dock at Highland Fabricator's Nigg yard in the north of Scotland, with the deck section built nearby at McDermott's yard at Ardersier. The TLP consists of a rectangular shaped floating platform connected to the ocean bottom by attaching 16 vertical tendons, four per corner column. The tendons are tensioned by attaching them to the floating structure and then deballasting the structure to provide additional buoyancy. The Hutton success has encouraged Conoco to proceed with development of several concepts for TLP suited to the milder environment and different production needs of the Gulf of Mexico.

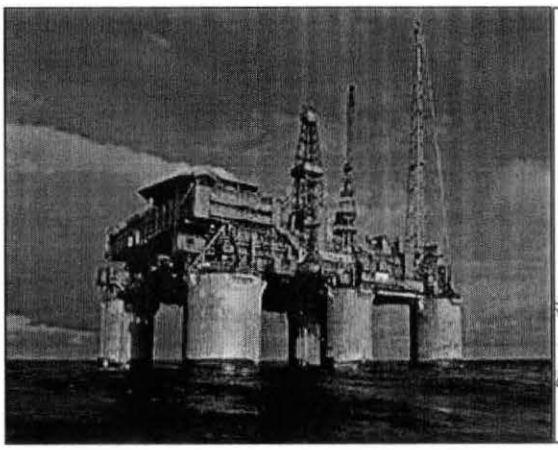

Figure 1.2 : Hutton TLP

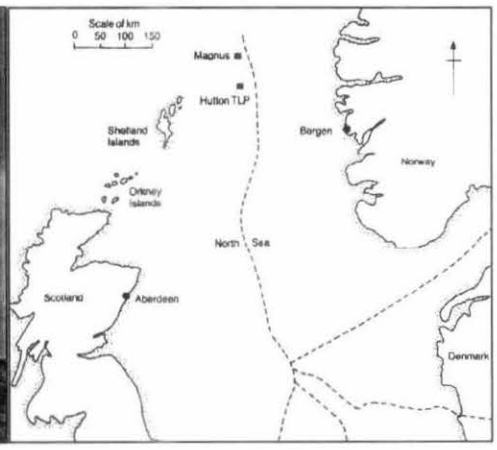

Figure 1.3 : Location Map of Hutton TLP

TLP in general has a lot of advantages over fixed offshore structures when oil exploration activity is moving towards deeper water. The total cost and complexity of fabrication, transportation and installation of fixed offshore structures at deeper water are the basis why multinational corporations in this field focus on floating structures. By statistics, the cost curves for fixed offshore structures will increase exponentially than the TLP. In addition, the reason for preferring TLP is that only the cost of mooring system and installation increases as the water depth increases.

TLP is essentially advantageous for the following reasons:

- TLP is a compliant structure thus it will respond well to wave loading and even to rough sea.
- The main natural frequencies (surge, sway and yaw) of TLP are well below the wave frequencies. As a result, it greatly reduces the possibility of occurrence of resonance. Furthermore, it also reduces the horizontal motion and loading on the tether's platform system.
- TLP can be easily dismantled, installed and transported according to site requirements.
- TLP is a much safer when responding to seismic activity compared with any other type of fixed platform.
- Risers, oil wells and tethers can be easily monitored and maintained due to its restrained vertical motion.

1.2 Problem Statement

Due to urbanization, the production of oil and other petroleum products have been rapidly increasing over the years. This has led to the scarcity of easily retrieved oil. As a result, oil producers are motivated to go to deeper ocean to extract oil and other resources. This interest in deep water drilling led to the in-depth study and analysis of deep water structures.

For this, deep water offshore structure such as TLP has become a main concern. TLP application for deepwater hydrocarbon exploration gives a very significant impact to

offshore field in term of engineering point of view and very economical. Furthermore, the economic impact can be further reduced by going through previously applied design approaches, to simplify the design and reduce the conservatism that so far has been incorporated in the TLP design.

According to Natvig and Vogel (1995), focus on design of future TLPs should be on the aspects of the platform geometry that affects tether loading and on the tether system itself. Their experience with a four-legged TLP has shown that the indeterminate tether system implies some very heavy cost items. The new concept of a three-legged TLP, which will be statically determinate, will not require complicated devices and the foundations can be placed with larger tolerances without affecting tether behavior. The main aspect of three-legged TLP is that all tethers share approximately the same loads despite weather directions. With the near-equal load sharing of the three-legged TLP, the maximum load level in one group is less, thus requiring less tether cross-section material than that of a four-legged TLP. Studies indicate that 12 tethers are feasible for a three-legged TLP whilst 16 would be required for a four-legged equivalent TLP. This is thus an important area for savings since tethers are important cost items.

Research on triangular TLP more or less will give different perception to offshore engineers where square TLP's are more preferred nowadays. In addition, results of this study can also be used to provide better solutions to problem due to vast changes in today's extreme environmental condition.

1.3 Objectives

- To conduct simple dynamic rigid body analysis in frequency domain for a typical triangular TLP subjected to random waves for determining the TLP motions.
- To conduct a parametric study of the above responses upon changing parameters like **significant wave height, water depth, draft** and **initial tether tension.**

1.4 Scope of Study

1.4.1 Project Data & Sea state

Due to rare application of Triangular TLP around the world, an actual scale model of triangular TLP idealized by Chandrasekaran and Jain (2000) from India is selected to be analyzed. The Triangular TLP model so called Reference Model in this thesis is built up of three vertical hulls and pontoons. Each hull of 16.39 m diameter has a length of 41 m of which 31 m of it is submerged below the Mean Sea Level (MSL). More details of the TLP is provided in figure 1.5.

Detailed frequency domain analysis is conducted by using Pierson-Moskowitz Spectrum concerning variation of parameters to investigate its effect on the dynamic response upon the TLP. The parameters include water depth, wave height, draft and initial pre-tension in the tethers. Pierson-Mostkowitz Sprectrum has been widely used by engineers to carry out response analysis of TLP because of its reliability in representing severe storm in offshore structures design.

1.4.2 Degree of Freedom

In reality, the combined environmental forces of wind, wave and current excites offshore structures, resulting in motion in six degrees of freedom. The oscillatory rigid body translation motions are referred to as surge, sway and heave, with heave being a vertical motion. The oscillatory angular motions are referred to as roll, pitch and yaw with yaw being rotation about the vertical axis (Faltinsen, 1993). The orientation of the platform relative to X, Y and Z axis and its motion in six degrees of freedom are shown in figure. 1.4.

The degree of motion of a structure depends on mooring stiffness, environmental loads, geometry, level of damping, etc. At this stage, the motion-response analysis

will only be focused on surge, heave and pitch degree of freedom as sea wave is assumed to be propagating towards (+)X-direction.

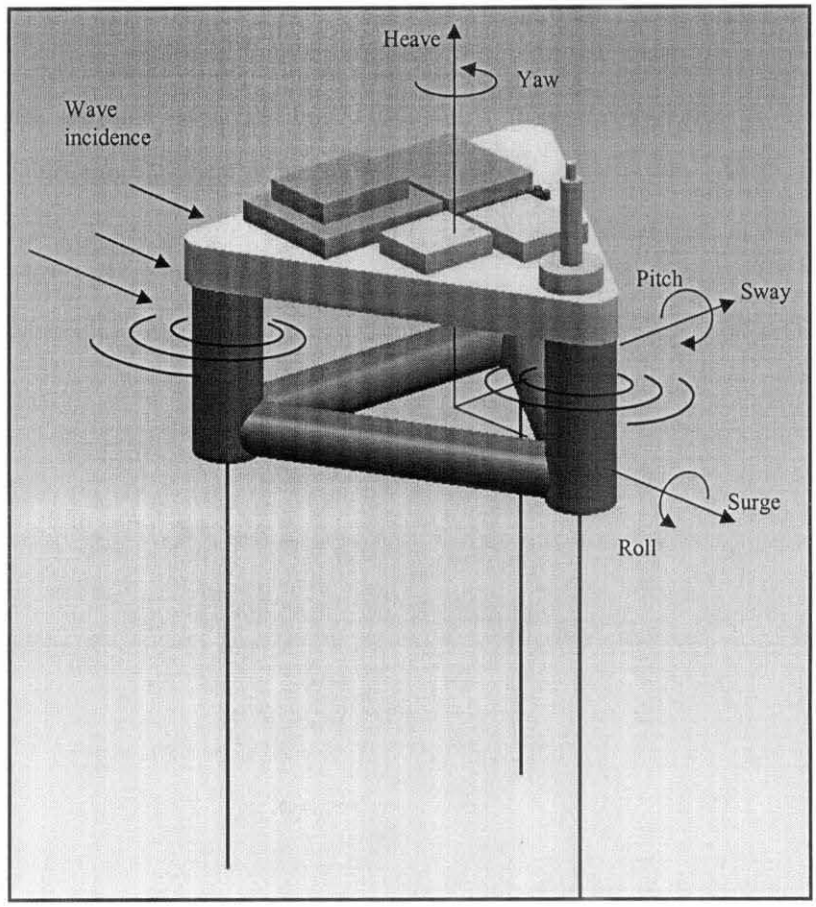

Figure 1.4 : Definition of rigid body motion modes

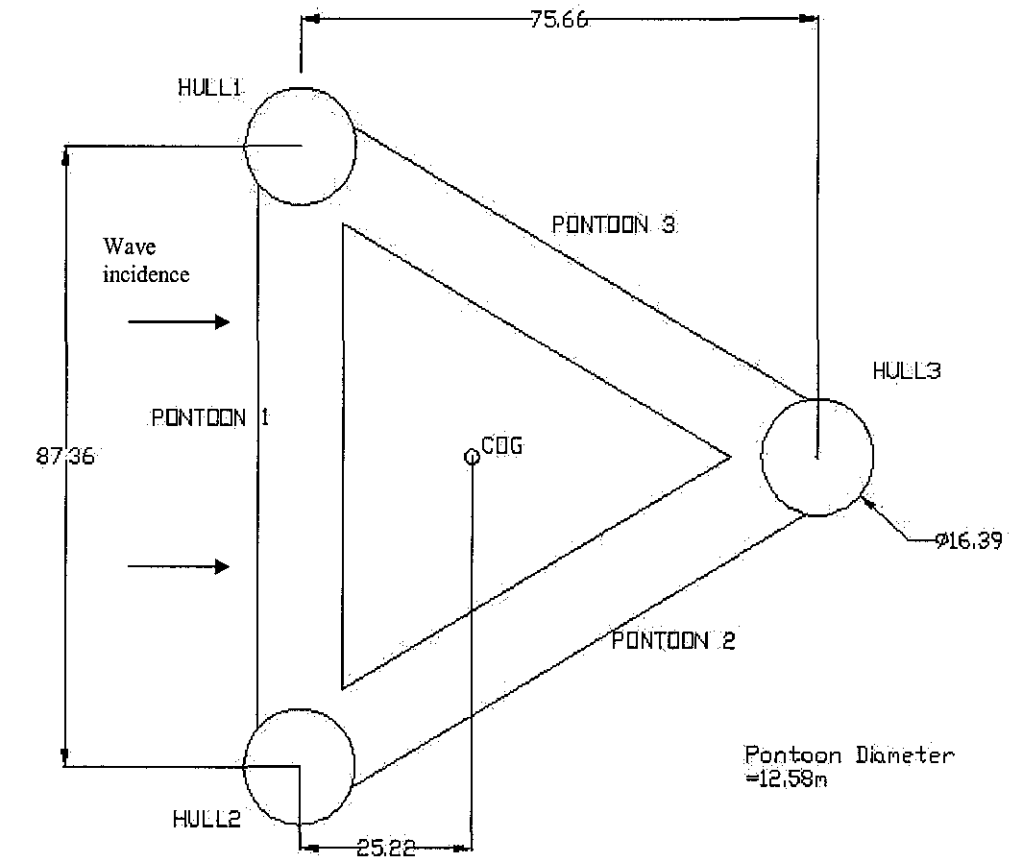

Figure 1.5 : Details of Triangular Tension Leg Platform

CHAPTER 2
LITERATURE REVIEW

2.1 Introduction

Nowadays, there are many TLPs in operation all over the world. Numerous studies have been done for effective application of TLPs for deep water oil exploration. These studies were carried out to obtain better understanding of the TLP structural behavior and dynamic response caused by changing parameters whilst improving the existing design.

2.2 Early Studies

Morgan and Malaeb (1983) investigated the dynamic response of TLPs using a deterministic analysis. The analysis was based on coupled nonlinear stiffness coefficients and closed-form inertia and drag-forcing functions using the Morison equation. The time histories of motions were presented for regular wave excitations. The nonlinear effects considered in the analysis were stiffness nonlinearity arising from coupling of various degrees of freedom, large structural displacements and hydrodynamic drag force nonlinearity arising from the square of the velocity terms. It was reported that stiffness coupling could significantly affect the behaviour of the structure and the strongest coupling found to exist between heave and surge or sway.

Chandrasekaran and Jain (2002a; 2002b) investigated the structural response behavior of the triangular TLP under several random sea wave loads and current loads in both time and frequency domains. They studied the effect of coupling stiffness coefficients in the stiffness matrix and the effect of water depth on the structural response of the triangular TLP.

Kurian et al. (1993) tested a 1:50 scale model of a square TLP in the laboratory in order to analyze its behavior when subjected to the action of regular and irregular waves. The experiment focused on surge, heave and sway degree of freedom for different angles of wave incidence.

Pauling and Horton (1970) came out with a method of predicting the platform motions and tether forces due to regular waves using linearized hydrodynamic synthesis technique together with several assumptions. The results of the analysis were compared until the results of laboratory tests. This study provided reliable results.

Angelides et al. (1982) considered the influence of hull geometry, force coefficients, water depth, pre-tension and tether stiffness on the dynamic responses of the TLP. The floating part of the TLP was modeled as a rigid body with six degrees of freedom. The tethers were represented by linear axial springs. Wave forces were evaluated using a modified Morison equation on the displaced position of the structure considering the effect of the free sea surface variation

Mekha et al. (1994) studied the nonlinear effect of the wave forces on the TLP up to the wave free surface. Several approximate methods were evaluated for regular and irregular wave forces, with and without current, and compared to Stoke's second order wave theory.

Force excitation upon the TLP hulls and pontoons require relevant wave theory to be applied. Preliminary stage of this project includes force calculation based on Linear Airy's Wave Theory or so called Small-Amplitude Wave Theory to obtain several wave parameters and later on Morison's equation for wave-force excitation.

2.3 Small-Amplitude Wave Theory

The earliest mathematical description of periodic progressive wave is that attributed to Airy in 1985. Airy wave theory is strictly only applicable to conditions in which the wave height is small compared to the wavelength and the water depth. It is commonly referred to as linear or first order wave theory, because of the simplifying assumptions made in its derivation.

This theory, developed by Airy (1845) is easy to apply, and gives a reasonable approximation of wave characteristics. This theory plays a vital role in this project as Morison's equation will be useful at the final stage of the wave force calculation.

Assumptions made in developing the linear wave theory are :

- The fluid is assumed to be homogeneous and incompressible (constant density).
- Surface tension can be neglected
- Pressure at the free surface is uniform and constant
- The fluid is ideal or inviscid.
- The particular wave being considered does not interact with any other water motion
- The bed is horizontal, fixed impermeable boundary, which implies that the vertical velocity at the bed is zero.
- The wave amplitude is small and the waveform is invariant in time and space.
- Waves are plane or long-crested (two –dimensional)

The basis for small amplitude wave theory is the sinusoidal wave and has already been classified based on relative water depth which are :

i. Deep water - $d/L > 0.5$

ii. Transitional water - $0.04 < d/L < 0.5$

iii. Shallow water - $d/L < 0.04$

These classification applies the same formula (general formula) to compute several wave parameters such as wavelength L, group velocity k, horizontal and vertical water particle velocity u and υ, and horizontal and vertical water particle acceleration u' and υ' respectively. For deep water region, the wave length is simply determined by :

$$L_o = L = \frac{gT^2}{2\pi} \tag{2.1}$$

The water particle velocity in the x and y direction are given by :-

Horizontal : $$u = \pi H \frac{\pi H}{T} \frac{\cosh ks}{\sinh kd} \cos\Theta \tag{2.2}$$

Vertical : $$\upsilon = \pi H \frac{\pi H}{T} \frac{\sinh ks}{\sinh kd} \sin\Theta \tag{2.3}$$

Then, the water particle accelerations in the x and y direction are given by :-

Horizontal : $$\frac{\partial u}{\partial t} = \frac{2\pi^2 H}{T^2} \frac{\cosh ks}{\sinh kd} \sin\Theta \tag{2.4}$$

Vertical : $$\frac{\partial \upsilon}{\partial t} = \frac{2\pi^2 H}{T^2} \frac{\sinh ks}{\sinh kd} \cos\Theta \tag{2.5}$$

where Θ = kx-ωt, phase angle

d, water depth	T, wave period
s, vertical distance from seabed	$\omega = 2\pi/T$, wave frequency
L, wavelength	$k = 2\pi/L$ wave number
H, wave height	t = time vary

These water particle velocity and acceleration will be further applied in Morisson's equation to compute wave loading upon the TLP.

2.4 Morison's Equation

The hulls and pontoons of TLP can usually be regarded as hydrodynamically transparent. The wave forces on the submerged members can therefore be calculated by Morison's equation, which expresses the wave force as the sum of an inertia force (proportional to the particle acceleration) and a non-linear drag force (proportional to the square of the particle velocity) as expressed in the equation below :

$$F = C_m \rho\pi D^2/4\, u' + C_d \rho D/2 |u| u \qquad (2.6)$$

Where;

C_m and C_d - Inertia and drag coefficient respectively

ρ - Seawater density

D - Diameter of cylindrical

u - Water particle velocity

u' - Water particle acceleration

In fact, the water particle velocity and accelerations are in its vector form (x, y and z). By using Morrison's Equation, there are several limitations and assumptions to be made :

- Analyzed section does not influenced by the adjacent sections flow.
- The cylinder is not piercing the free surface.

2.5 Pierson-Moskowitz Spectrum

Irregularity in sea waves make it very difficult to be generated and used in analysis. However, there is a solution to take into account the irregularity of the waves, by determining the total energy. In order to do this, the energy of all the small, regular and large waves superposed in the sea waves must be added together. Therefore, any given waves can be described by the energy distribution vs the different frequencies (or wave lengths or wave periods) for various wave components. This frequency distribution is called the energy spectrum for the particular sea.

The spectral density of the sea surface elevation is completely characterized by significant wave height, H_s and average time period, T_s. Although the wave pattern will never be repeated, the statistical characteristics of the sea-state, the energy spectrum or wave spectrum, will remain the same. As a result Pierson-Moskowitz Spectrum, one of wave spectra was introduced.

The Pierson-Moskowitz Spectrum was developed from analysis of measured data obtained in the North Atlantic by Tucker wave recorders installed on weather ships. The analysis only considers selected wave records that represent fully developed seas (for wind speed between 20 and 40 knots). The wind speed is recorded at an elevation of 19.5 m.

Nowadays, the P-M model has been found to be very useful and most reliable in representing a severe storm wave in offshore structure design. This spectrum model is written as :

$$S(f) = \frac{0.0081g^2}{(2\pi)^4} f^{-5} exp\left[-1.25\left(\frac{f}{f_o}\right)^{-4}\right] \qquad (2.7)$$

From P-M model, the height of wave at a particular frequency can be calculated. For example, at a frequency f_1, the energy density is $S(f_1)$. The wave height at this frequency is obtained as follow :

$$H(f_1) = 2\sqrt{2S(f_1)\Delta f} \tag{2.8}$$

and the corresponding wave period is given by :

$$T = \frac{1}{f_1} \tag{2.9}$$

Where (H,T) is the wave height-period pair. A phase angle associated with each pair of height and period is chosen uniformly distributed in the range of $(0, 2\pi)$ by a random number generator, R_N as :

$$\varepsilon(f_1) = 2\pi R_N \tag{2.10}$$

Then, for a given horizontal coordinate, x, which is the location at which the wave profile is desired, and time, t, is incremented to get the wave profile. The wave profile is computed from :

$$\eta(x,t) = \sum_{n=1}^{N} \frac{H(n)}{2} \cos\left[k(n)x - 2\pi f(n)t + \varepsilon(n)\right] \tag{2.11}$$

Where $k(n) = 2\pi/L(n)$ and L(n) corresponds to the wave length for the n^{th} frequency, f(n). The quantity, N, is the total number of frequency bands of width, Δf, dividing

the total energy density. An example of wave spectra for different wind speeds is provided in figure 2.1.

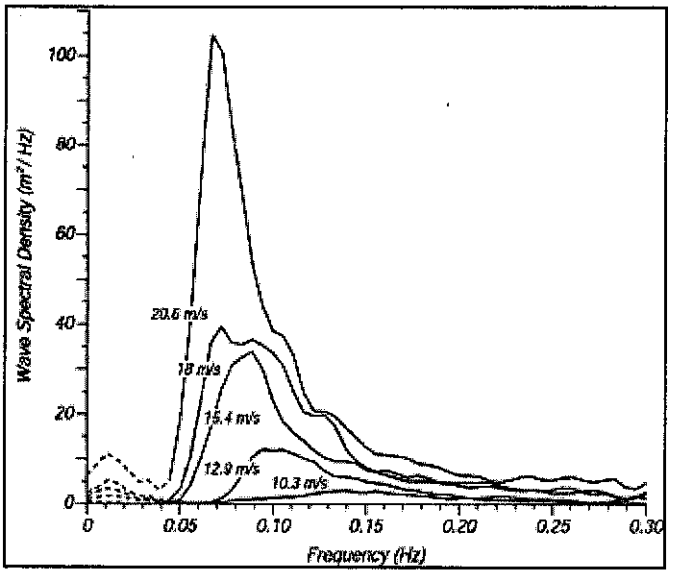

Figure 2.1 : Wave spectra of a fully developed sea for different wind speeds according to Moskowitz (1964).

2.6 Response Amplitude Operator

The amplitude of the response of TLP is generally normalized with respect to the amplitude of the wave. For a given linear system, the normalized response is constant with the wave amplitude at a wave frequency. But if a normalized response function is developed for a range of frequency of interest for a given offshore structures, then this function is called Response-Amplitude Operator (RAO) because it allows the transfer of the exiting waves into responses of the structure.

In general, RAO can be obtained theoretically or by measurement. Theoretical RAO is represented by the term in bracket in the displacement function as discussed in following section. For simplification, response is briefly described as follow:

$$\text{Response (t)} = (\text{RAO})\,\eta(t) \tag{2.12}$$

where $\eta(t)$ is the wave profile as a function of time, t.

2.7 Motion-Response Spectrum

When a structure is dynamically loaded by waves, it will result in motions. The motions may be critical near the resonant frequency of the structure. The effect of resonance is undesirable as it can cause the collapse of the structure. Thus, it is important to study the overall response of the structure according to design-wave spectrum. In this case, the response-amplitude operators (RAOs) are implemented relating the dynamic motion of the structure to the wave-forcing function. Then the dynamic-motion spectrum is obtained from the wave spectrum and eventually the motion profile can be easily generated.

The displacement function x(t) or motion of the structure in a particular direction, e.g., surge, sway, heave can be written as :

$$x(t)=\left[\frac{\frac{F_I}{0.5H}}{[(K-m\omega^2)^2+(C\omega)^2]^{\frac{1}{2}}}\right]\eta_\beta(t) \tag{2.13}$$

where β is the phase difference between x(t) and $\eta(t)$. This relationship can be transformed to obtain the motion spectrum in terms of the wave spectrum and RAO (terms inside the bracket).

$$S_x(f)=\left[\frac{\frac{F_I}{0.5H}}{[(K-m\omega^2)^2+(C\omega)^2]^{\frac{1}{2}}}\right]^2 S(f) \tag{2.14}$$

Where,

F_I – Total wave forces

H – Wave height

K – Stiffness of the TLP (K_{surge}, K_{heave} and K_{pitch})

m – Total mass of the TLP (m_{surge}, m_{heave} and m_{pitch})

The total mass of TLP in surge, heave and pitch are given as

$$m_{surge} = m_{TLP} + \left[3V_H + V_p + 2\left(V_p \cos 60 + \frac{\pi D_p^3}{12}\cos 30\right)\right]\rho \quad (2.15)$$

$$m_{heave} = m_{TLP} + \left[3V_p + \frac{3\pi D_H^3}{12}\cos 30\right]\rho \quad (2.16)$$

$$m_{pitch} = m_{heave} \times r_z^2 \quad (2.17)$$

While stiffness of the TLP, K in surge, heave and pitch are given as

$$K_{surge} = 3\,T_0 / L_T \quad (2.18)$$

$$K_{pitch} = \omega_{pitch}^2 \times m_{pitch} \quad (2.19)$$

$$K_{heave} = (\text{No. of tethers} \times K_{tether}) + (3\rho g V_H) \quad (2.20)$$

Where,

m_{TLP}	-	Mass of TLP	L_T	-	Length of tether
T_o	-	Initial Tether Tension	V_P	-	Volume of pontoon
g	-	Gravitational acceleration	V_H	-	Volume of hull
D_P	-	Diameter of pontoon	K_{tether}	-	Stiffness of tether
D_H	-	Diameter of hull	r_z	-	Radius of gyration

CHAPTER 3
METHODOLOGY

3.1 Introduction

The objective of this project is to study the responses of triangular TLP subjected to random waves. A frequency domain analysis was used to obtain the responses. The following methodology was adopted. Important parameters which include structural dimension and sea state were identified. This was followed by the wave force calculation, and the wave and motion spectrum development. For parametric study, several cases of analysis for significant wave height, water depth, initial tether tension and draft are established.

3.2 Identification of Important Parameters

The sea state applied in this project is obtained from previous research by Chandrasekaran & Jain (2000). Significant wave height and water depth are then divided to several cases to study its effect on the TLP response.

Wave parameters

Significant Wave height, H_s	:	8	m
Wave period, T	:	12	sec
Water depth, d	:	300	m
Water density, ρ	:	1030	kg/m3
Drag coefficient, C_d	:	1	
Inertial coefficient, C_m	:	2	

TLP Properties

TLP dimension has been described in detail in the earlier section of this report. The remaining are provided as follow :

Weight	: 330000 kN		Damping ratio, ζ	:	0.01
Stiffness of Tether, K_{tether}	: 34000 kN/m		Design Life	:	20 years
Initial Tether Tension, T_o	: 135500 kN		Diameter, D_H	:	16.39 m
Tether Length, L_T	: 269 m		Length , L_H	:	31 m
CoG Above Keel	: 27.47 m		Diameter, D_P	:	12.58 m
r_x	: 35.1 m		Length, L_P	:	70.97 m
r_z	: 35.1 m				

3.3 Wave Force Calculation

After the respective parameters are identified, computation of wave forces was started with Airy's wave theory followed by Morison's equation. The steps are provided in figure 3.1.

Detailed dimension of TLP described in figure 4 includes the structure COG, height and dimension of draft, pontoons and hulls diameter, and TLP total mass. The COG of the structure was chosen to be at the origin of the global coordinate system.

Airy's wave theory implementation was started by firstly identifying the water condition. This step is to ensure that the TLP to be analyzed is operating in deep water condition. After that, water particle velocity and acceleration was computed based on sea state available. However the water particle velocity and acceleration has to be decomposed into components of three orthogonal directions. Then, the force vector in this case could be obtained by applying drag and inertia coefficient together with components of velocity and acceleration into the Morison's equation.

Morison's equation was evaluated by using the Microsoft Excel. Moment was calculated with respect to COG of the structure. As the structure is analyzed in Single Degree of Freedom, only moment about y-axis was calculated. The spreadsheet developed towards the computation of the wave forces and moment is given in Appendix.

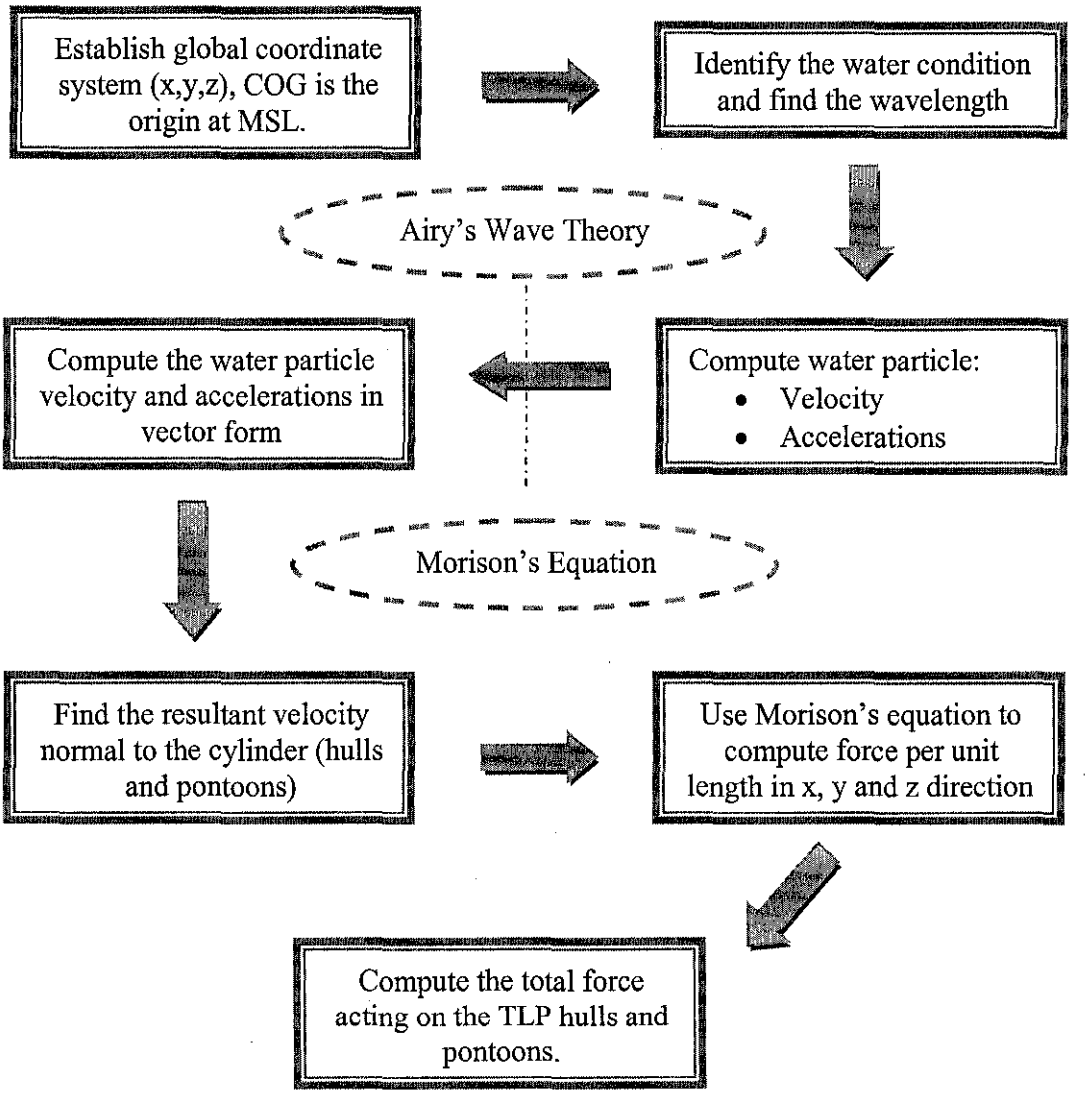

Figure 3.1 : Steps for wave force calculation

3.4 Wave and Motion Spectrum Development

Next, P-M Spectrum was developed based on a specified significant wave height, H_s. Frequency, f, ranging from 0.02 Hz to 0.22 Hz with equal increment was considered in the development of this curve. After that, a period of random wave profile, η, at a incremented time, t can be generated.

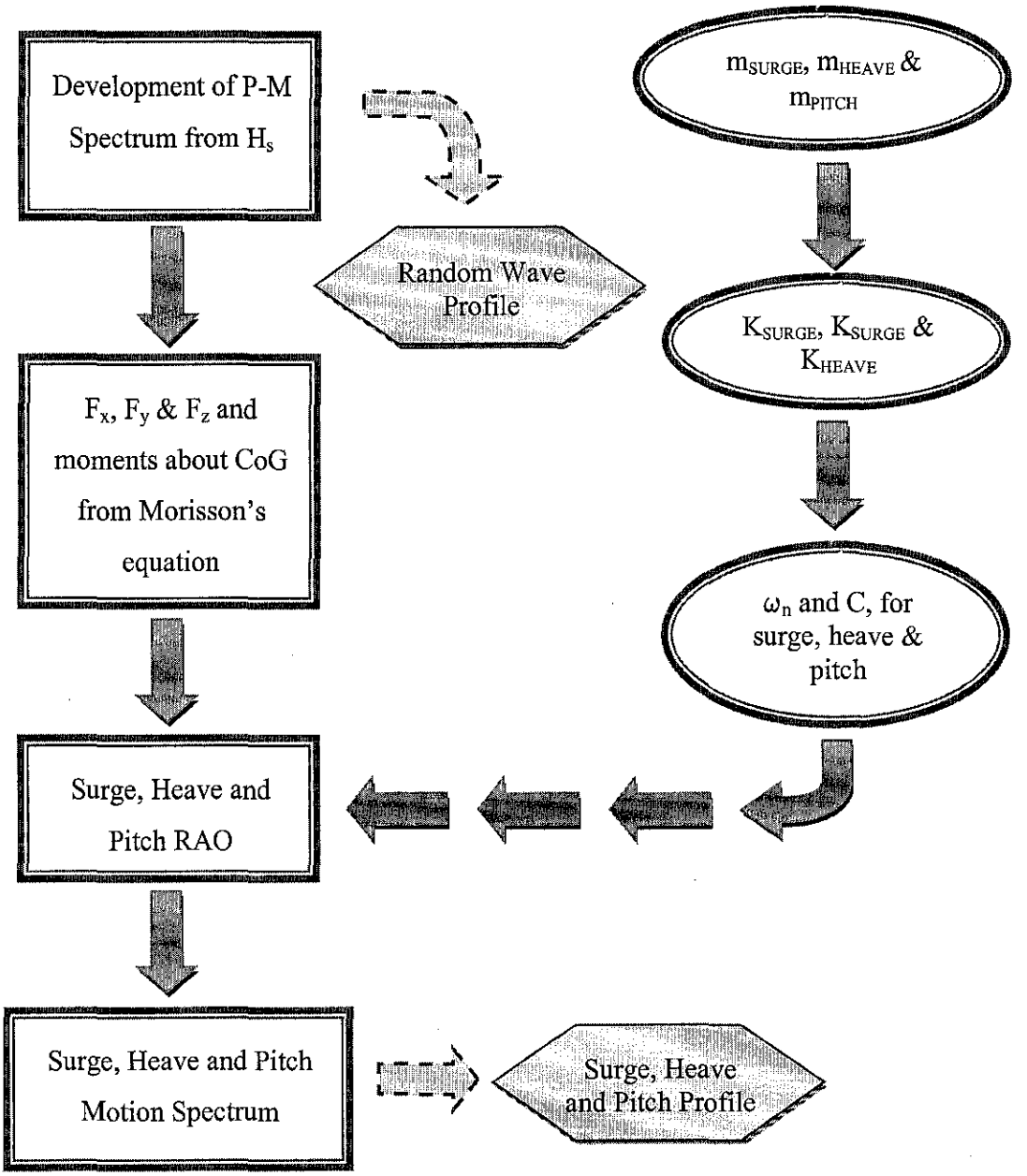

Figure 3.2 : Steps of computing motion RAO

At later stage, the energy density spectrum was used to develop the motion spectrum in surge, heave and pitch motion of the triangular TLP. Motion profile was also generated in a way similar to the random wave profile was generated. Numerical calculation was made by using Microsoft Excel program.

The response of the TLP at a range of frequency could be calculated by substituting force components obtained from the Morison's equation together with the structure mass and stiffness for respective analyzed motion (surge, sway and heave) into response formula.

3.5 Parametric Study

The parametric studies were conducted to compare the response of the proposed triangular TLP under different wave height, water depth, draft and initial tether tension. The Reference Model was used as a base for various ranges of cases as shown in Table 3.1, 3.2, 3.3 and 3.4.

Table 3.1 : Study of triangular TLP subjected to different significant wave height

Case	Significant Wave height, H_s	Wave Period T
Case 1A	6	12
Case 1B	8	12
Case 1C	10	12
Case 1D	12	12

Table 3.2 : Study of triangular TLP at different water depth, H_s = 8m, T= 12 sec

Case	Water Depth m
Case 2A	300
Case 2B	600
Case 2C	900
Case 2D	1200

Table 3.3 : Study of triangular TLP with different drafts, H_s = 8m, T= 12 sec

Case	Draft m
Case 3A	25
Case 3B	31
Case 3C	35
Case 3D	40

Table 3.4 : Study of triangular TLP with different initial tether tension, H_s = 8m, T= 12 sec

Case	Weight kN	Initial Tether Tension kN
Case 4A	300 000	165 000
Case 4B	330 000	135 500
Case 4C	360 000	105 500
Case 4D	390 000	75 500

3.6 Hazards Evaluation

Students are vulnerable to a number of health hazards when doing computer analysis repetitively. The principal hazard relates to the arms. The problems which can develop are referred to as WRULDs (work related upper limb disorders) or RSI (repetitive strain injuries). Applying ergonomic principles to the design, selection and installation of computer equipment and the design of the workplace can readily control the risks.

Computer-related injuries and illnesses can be avoided with some simple ergonomically wise applications:

- Workstation is arranged to ensure comfortable workspace and do not cause unnecessary strain on the back, arms or neck.
- Monitor display is equipped with monitor visor to filter excessive amount of light intensity that can cause eye strain.

- Ergonomic keyboard and mouse is installed to reduce palms and arms strain.
- Computer is placed on a standard-height desk that is specifically designed for its use.
- Workstation is equipped with comfortable chair with good back and arm support.
- Keyboard is positioned directly in front of student at approximate elbow height.
- Breaks are taken at a specific time period to perform some stretch such as get up and moving around.
- To avoid falls and injuries, stored item is not placed on top of tall cabinets or furniture.

CHAPTER 4
RESULTS AND DISCUSSIONS

4.1 Introduction

The numerical results obtained from calculation by using Excel spreadsheet are divided in the following sections. The first part of this chapter will generally discuss about the generated random waves from the energy spectrum and the wave forces exerted on the TLP. Then, the next section will discuss about the parametric study that has been considered in this project

4.2 Random Waves, Wave Forces and TLP Response

Numerical results from Airy's Wave Theory and Morison's Equation which correlate water particle velocity and acceleration produce total wave force exerted on triangular TLP. A sample of wave force distribution along a triangular TLP draft is shown in figure 4.1. It appears that wave forces exerted along the TLP draft is decreasing exponentially as it moving deeper towards the keel.

P-M model developed from significant wave height, H_s = 8m produce a bell shape curve as presented in figure 4.2. The starting frequency is 0.02 Hz. The energy density increases rapidly as wave frequency increases until it reaches the peak at approximately 0.08 Hz. The energy density declines beyond this frequency of wave. High energy density indicates wave of that particular frequency dominated the location where the data was recorded.

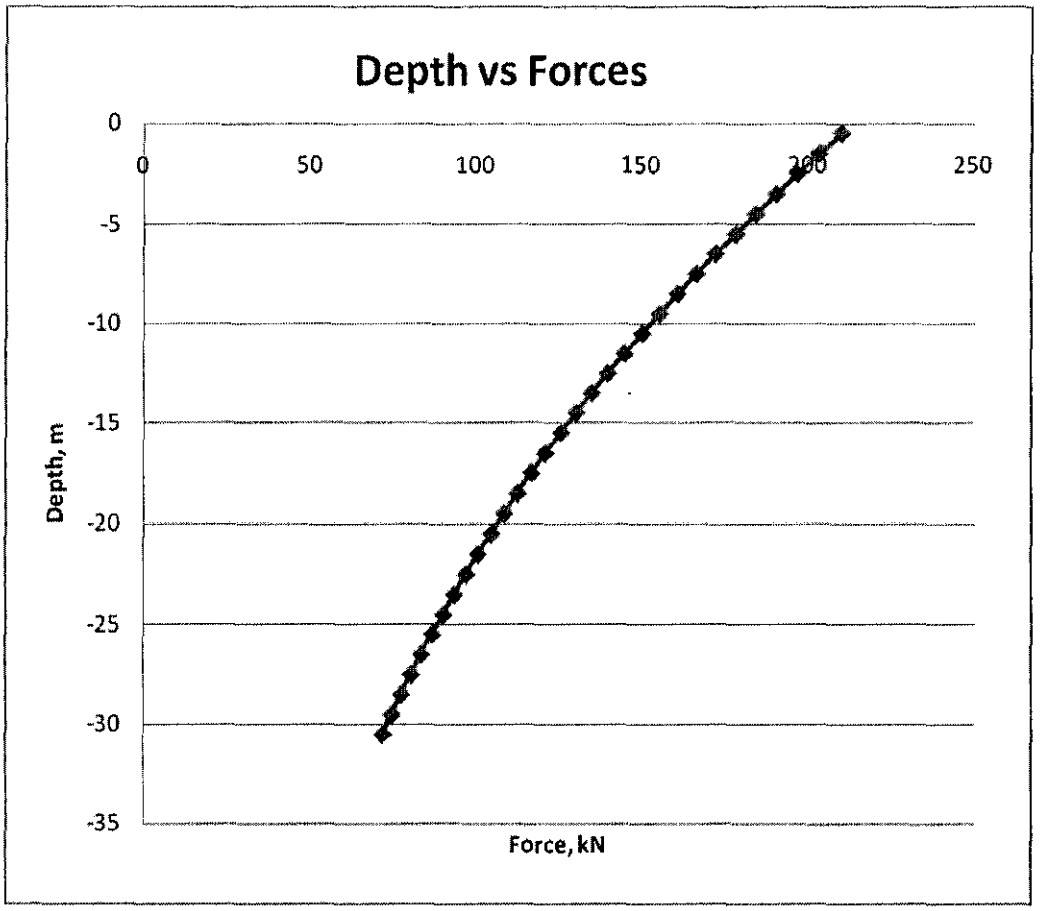

Figure 4.1 : Water depth versus wave forces (Hull 1 & 2)

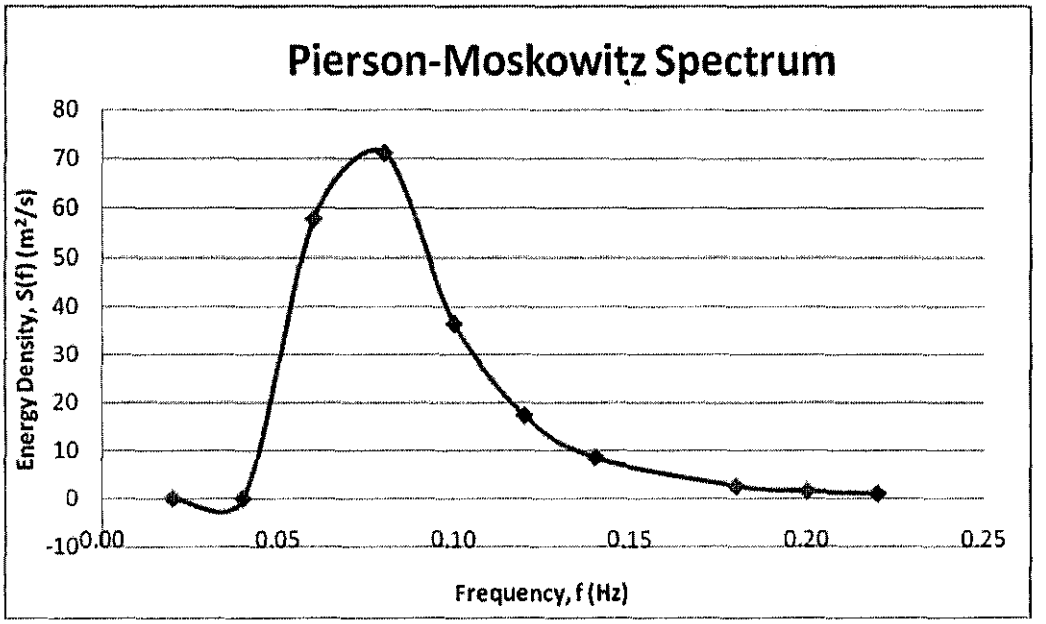

Figure 4.2 : Pierson-Moskowitz Spectrum

Generally, random waves govern the wave profiles in open sea. Random waves consist of a number of sinusoidal waves of different wave lengths and heights that are superimposed on each other. The indefinite pattern of random waves in reality could come from any direction and also never repeated from one time to another. An example of random waves generated from P-M spectrum of 8 m significant wave height is shown in figure 4.3.

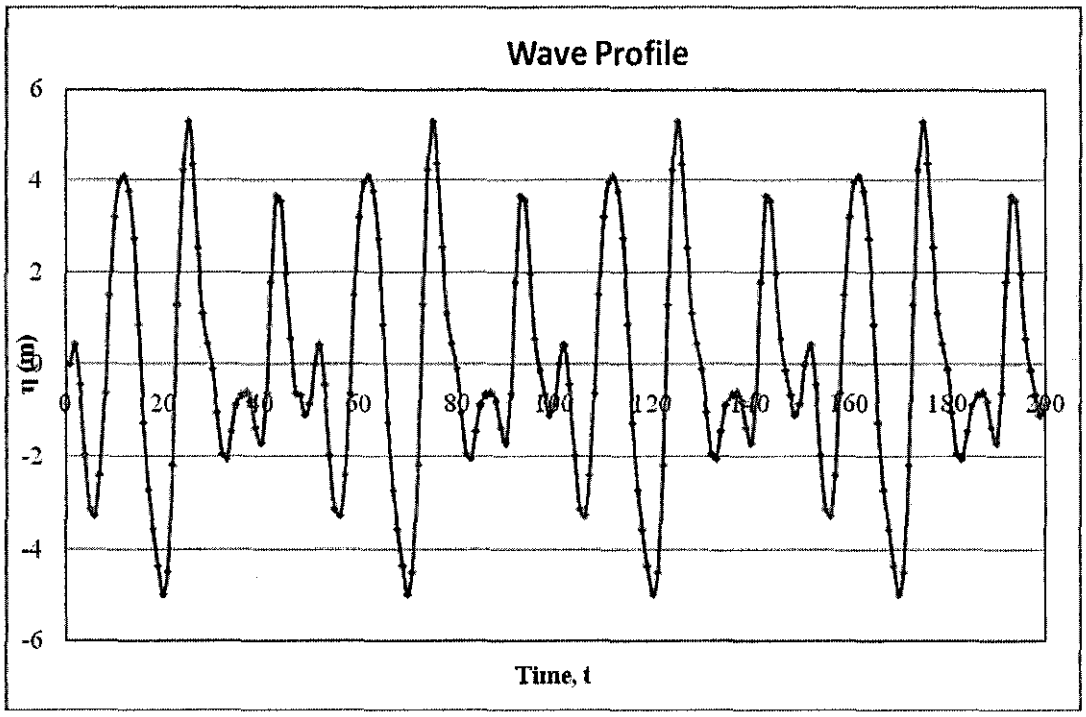

Figure 4.3 : Wave Surface Profile

Similarly, motion spectrum obtained was used to generate surge and heave profile. Both profile show random pattern of line as a response of random waves excite the TLP. Surge and heave profile produced in figure 4.4 and figure 4.5 respectively were based on H_s = 8 m of and T = 12 sec.

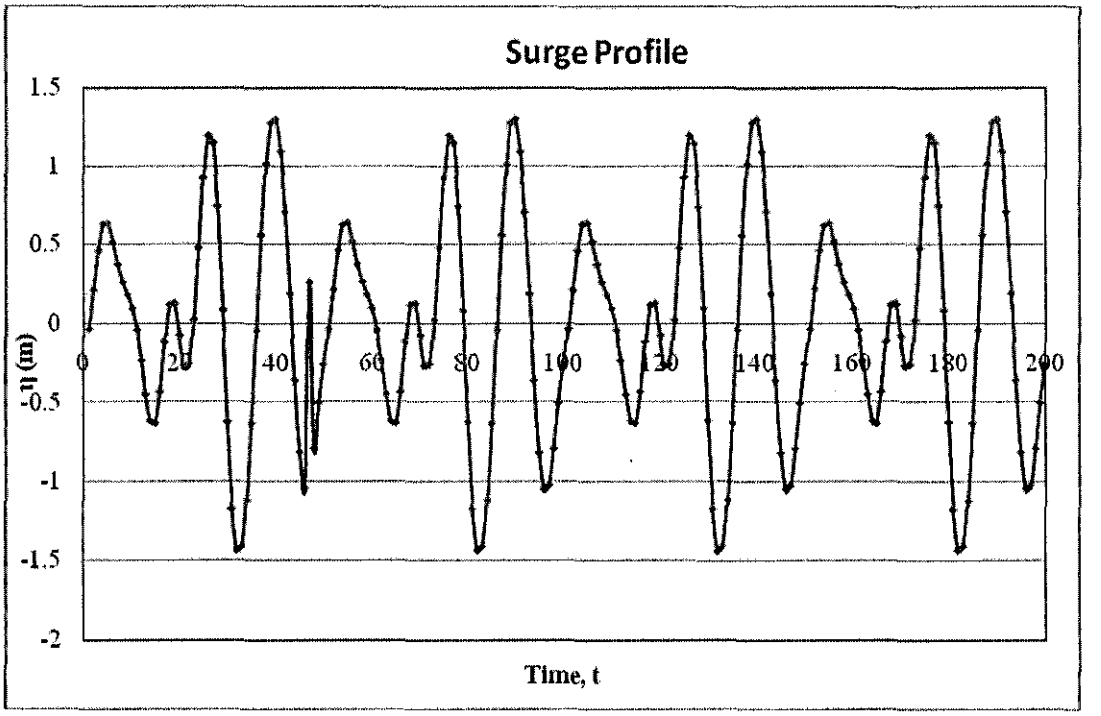

Figure 4.4 : Surge Profile

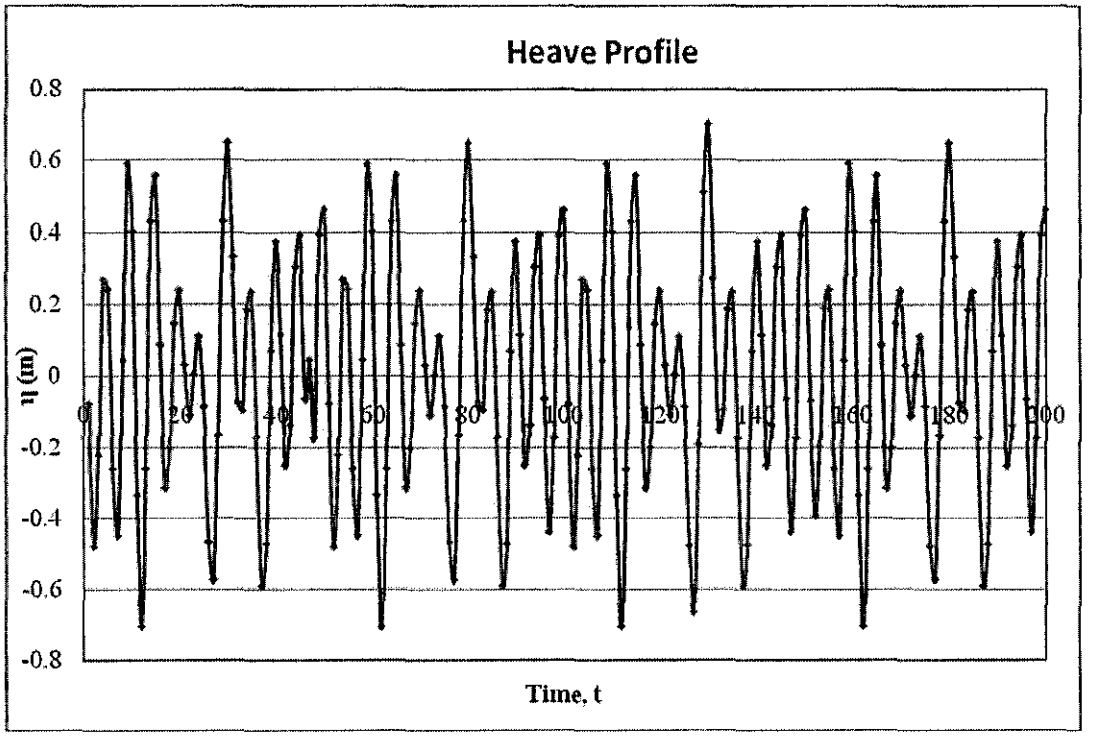

Figure 4.5 : Heave Profile

4.3 Parametric Study

4.3.1 Effect of Significant Wave height

Waves approaching the triangular TLP have significant impact on the structure response. Usually greater wave height results in greater response of the structure but it also depends on the tether stiffness, total mass and damping coefficient of the triangular TLP.

Figure 4.6 shows the surge RAO at different significant wave height, H_s. It is found that different significant wave heights give minute effect on TLP surge RAO. The surge RAO at 0.02 Hz is very large (3.5) compared to other wave frequency due to very small wave height formed by the other range of frequency. However, surge motion spectrum as shown in figure 4.7 is highest at 0.06 Hz given by H_s = 12 m.

Figure 4.8 shows that the variation of heave RAO at different significant wave heights, H_s are similar to each other (superimposed lines). Maximum RAOs are mostly located at 0.20 Hz. The highest heave RAO is around 0.20 for all H_s's. Heave motion spectrum gives it highest value of 4 at 0.20 Hz for all H_s's.

Table 4.1 shows the maximum pitch response of triangular TLP resulted from different maximum wave height, H_{max}. The pitch response of the TLP increases as the H_{max} resulted from the respective significant wave height increases.

Table 4.1 : Maximum pitch response subjected to different H_{max}

H_s (m)	H_{max}, (m)	T (sec)	Pitch (degree)
6	18.1	12	-0.07
8	24.4	12	-0.10
10	30.4	12	-0.12
12	35.8	12	-0.15

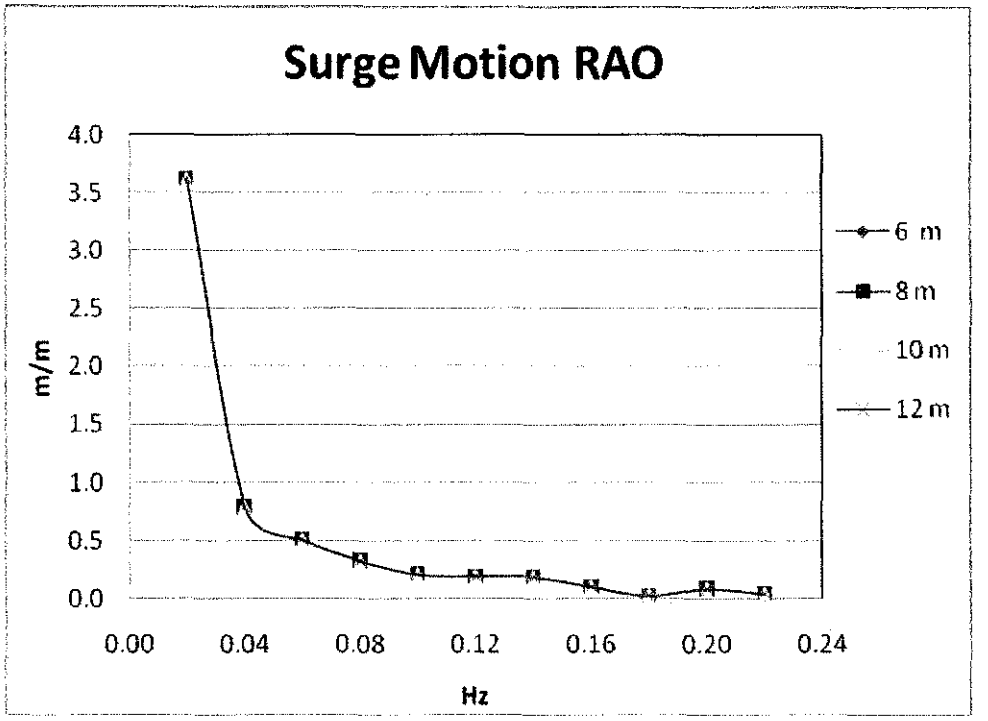

Figure 4.6 : Surge Motion RAO for various significant wave height, H_s

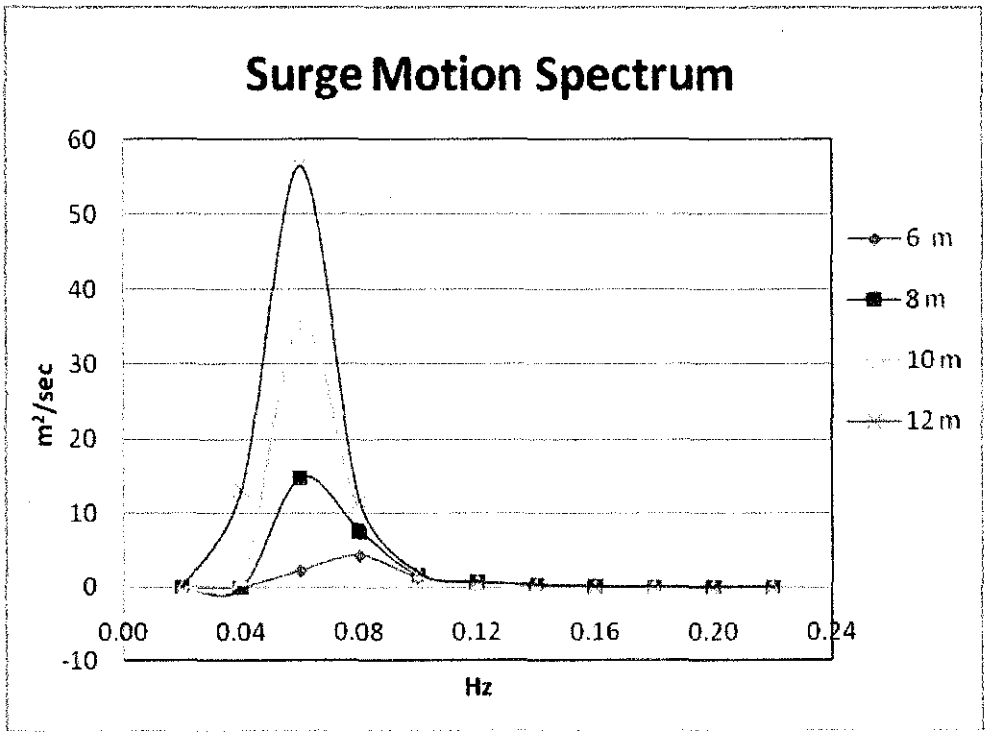

Figure 4.7 : Surge Motion Spectrum for various significant wave heights, H_s

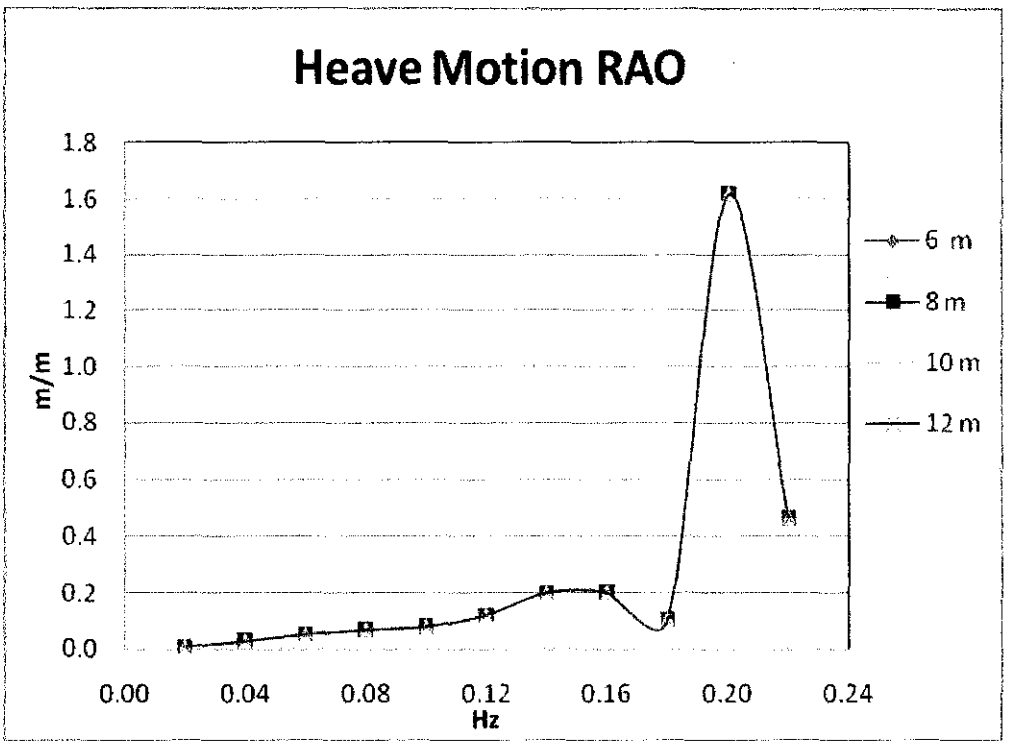

Figure 4.8 : Heave Motion RAO for various significant wave heights, H_s

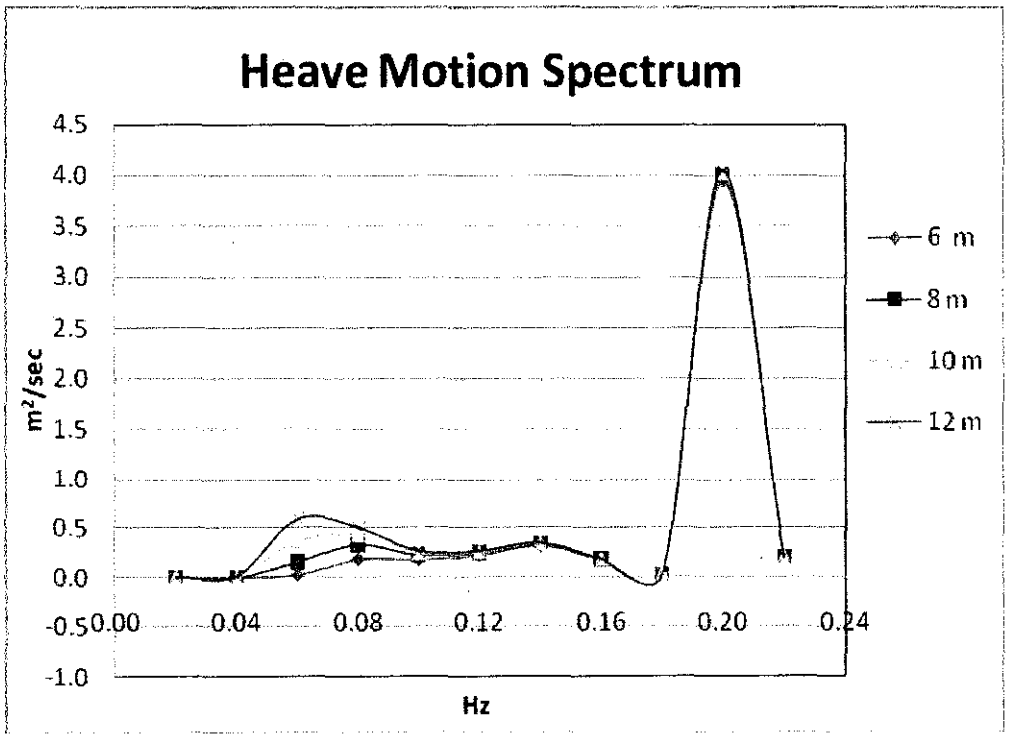

Figure 4.9 : Heave Motion Spectrum for various significant wave heights, H_s

4.3.2 Effect of Water Depth

It is also important to study the effective of changing water depth on forces acting on triangular TLP when it is subjected to random waves. As far as deep water oil and gas exploration is concerned, TLP application has become very popular due to its compliant nature when operating at great water depth. In this part, the triangular TLP was analyzed to be operated at 300 m, 600 m, 900 m and 1200 m water depth. Thus, this study has resulted in longer tether length as other parameters are kept constant.

From Figure 4.10 and 4.11, the surge RAO and surge motion spectrum are highest at 300 m water depth. High value of RAO at 0.02 Hz means that resonance is expected to occur, where the frequency of the TLP is close to the frequency of wave. In real case of offshore structure design, 0.02 Hz wave frequency will be omitted from being analyzed hence resonance could be avoided. Figure 4.11 shows surge motion spectrum at different water depth. Highest energy density for each water depth is produced at 0.06 Hz.

Figure 4.12 and 4.13 represents heave RAO and heave motion spectrum respectively. Both figures show similar pattern of lines and values respectively (superimposed lines). Greatest value of heave RAO is given by 1.6, while the respective energy density is 4 m^2/sec at 0.2 Hz.

Table 4.2 shows the maximum pitch response of triangular TLP under different water depth at H_s = 8 m. All in all, water depth variation does not largely influence the response (surge, heave and pitch) of the triangular TLP.

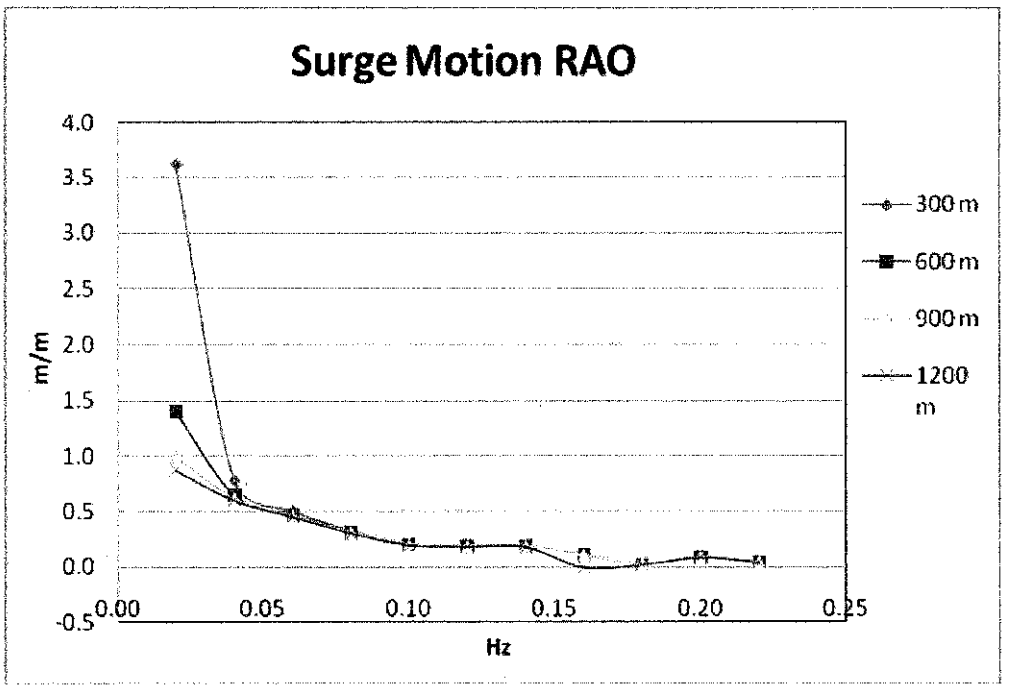

Figure 4.10 : Surge Motion RAO for different water depth

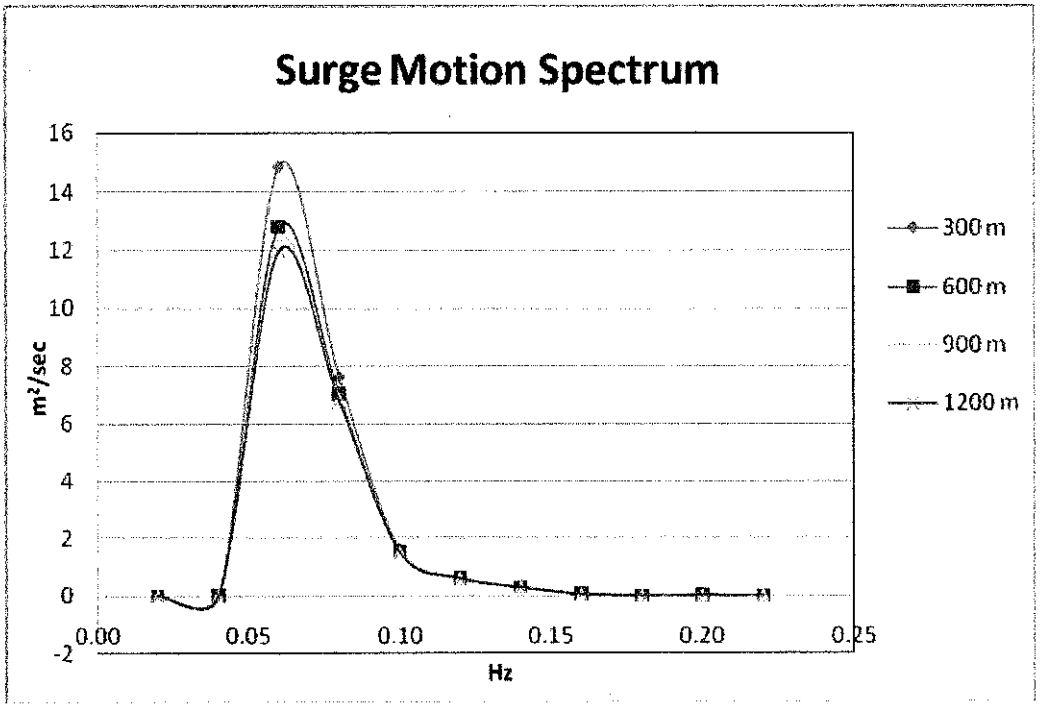

Figure 4.11 : Surge Motion Spectrum for different water depth

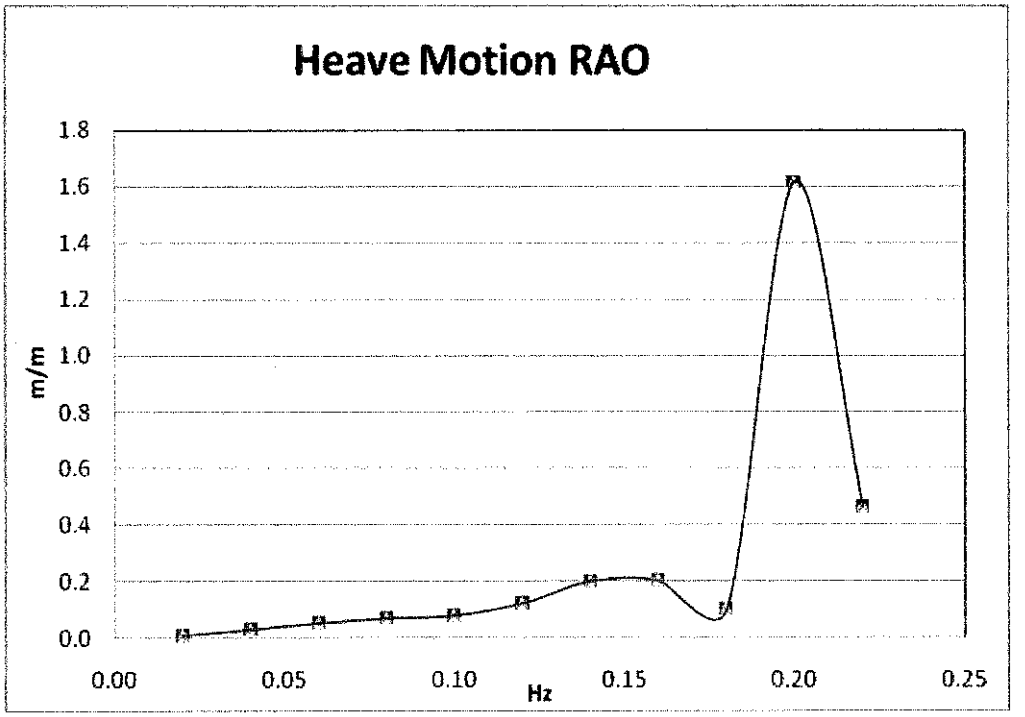

Figure 4.12 : Heave Motion RAO for different water depth

(300 m, 600 m, 900 m and 1200 m)

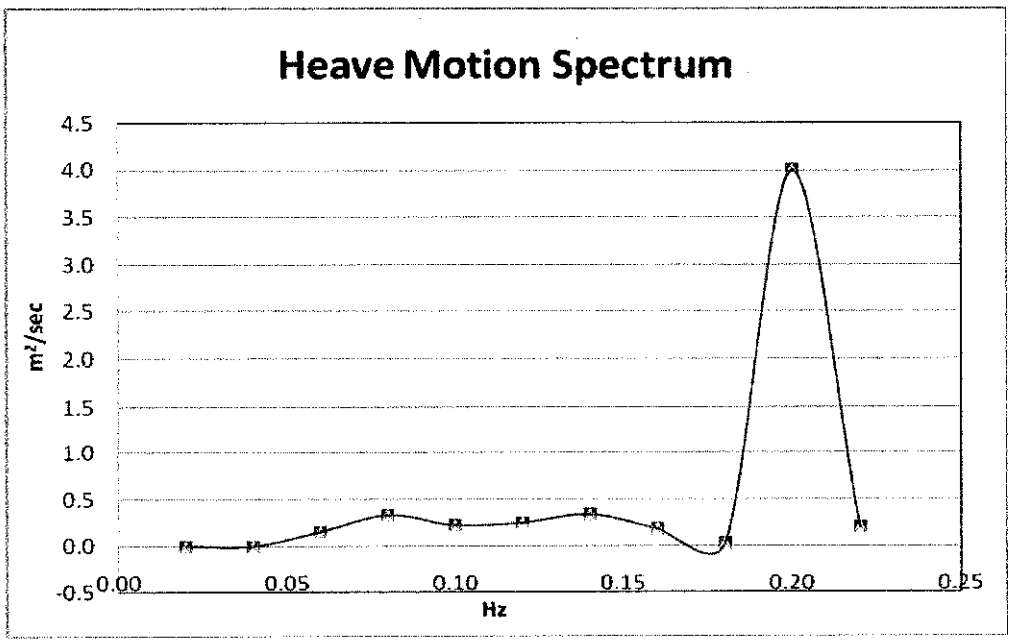

Figure 4.13 : Heave Motion Spectrum for different water depth

(300 m, 600 m, 900 m and 1200 m)

Table 4.2 : Maximum pitch response at different water depth

Water depth (m)	H_{max}, (m)	T (sec)	Pitch (degree)
300	24.4	12	-0.10
600	24.4	12	-0.10
900	24.4	12	-0.10
1200	24.4	12	-0.10

4.3.3 Effect of Draft

Changing draft is one of the studies concerned in the TLP dynamic analysis. Due to variable draft, the buoyancy force as well as mass in the respective motion changes. Water particle velocity and acceleration near SWL also vary appreciably. Figure 4.14 and 4.16 show the RAO (surge and heave) of TLP under different draft of the TLP.

Surge motion RAO is greatest when the TLP draft is 25 m, as shown in figure 4.14. The respective RAO value is 4.5 at 0.02 Hz wave frequency. 31, 35 and 40 m draft also have highest surge RAO at this frequency. The lines of RAO of different drafts become similar to each other beyond 0.04 Hz.

Surge motion spectrum shows bell-shape lines for all drafts. All drafts have highest energy density at 0.06 Hz. The highest energy density is resulted from 25 m draft, $15m^2$/sec. The heave motion under variable draft is highest at 0.2 Hz for all draft. The respected energy density is 4 m^2/sec. Heave response does not significantly affected by changing TLP draft.

Table 4.3 shows the maximum pitch response of triangular TLP by varying triangular TLP draft. The pitch response was analyzed for H_{max} resulted from H_s = 8 m. Pitch response increases from 25 m to 35 m of draft. The response declines when the draft is 40 m.

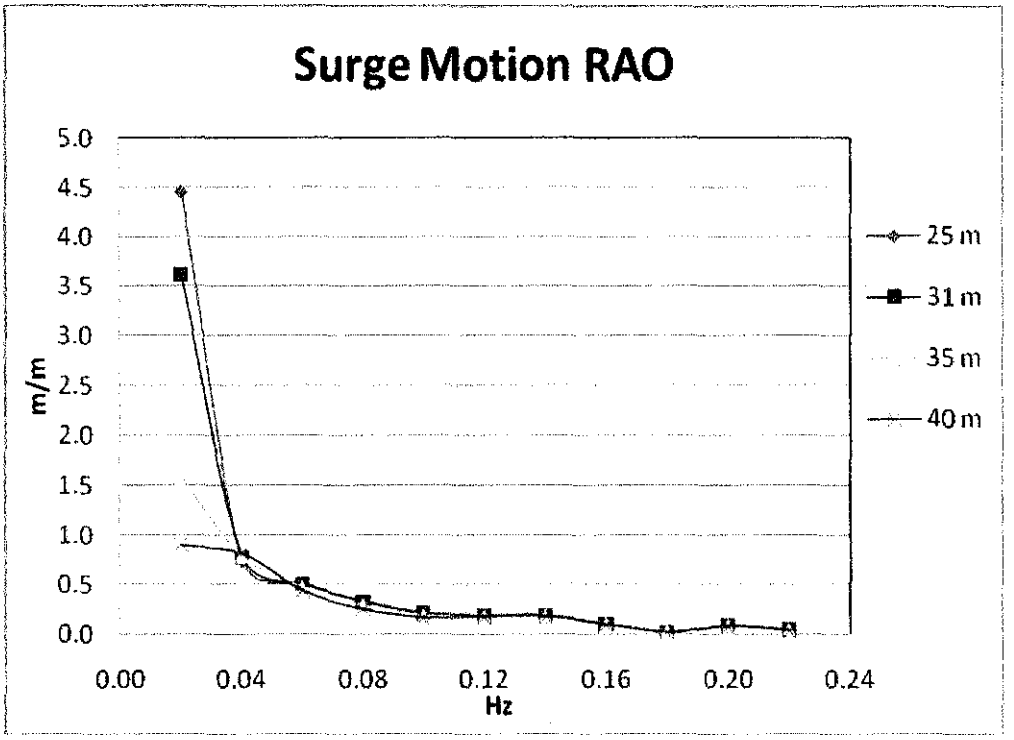

Figure 4.14 : Surge Motion RAO by varying triangular TLP draft

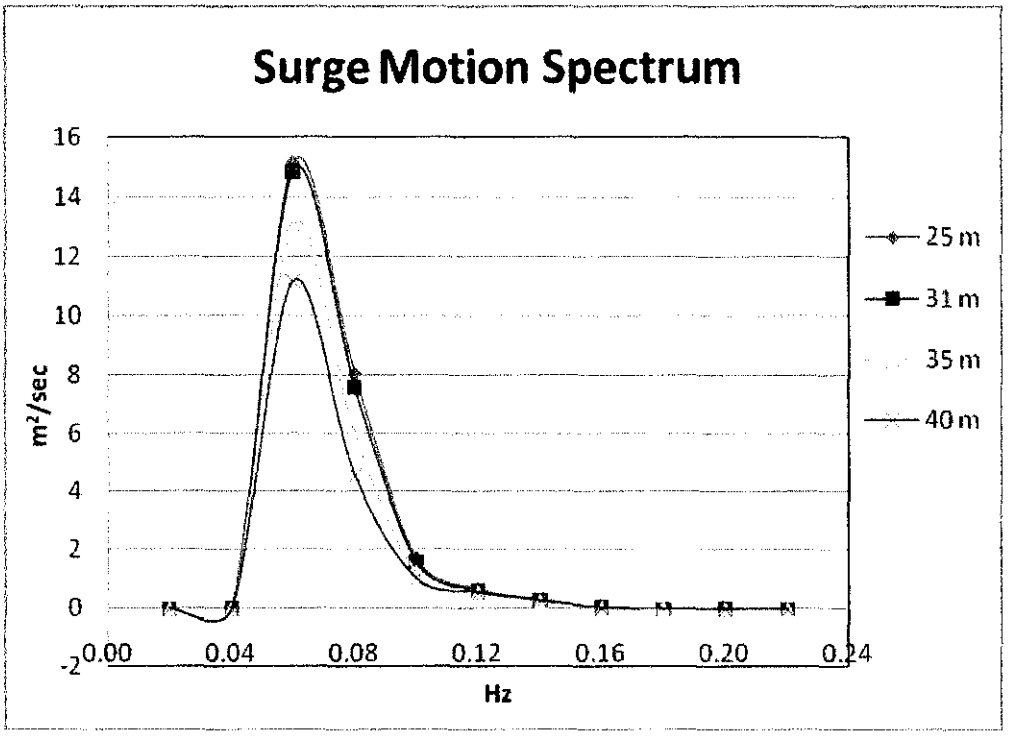

Figure 4.15 : Surge Motion Spectrum by varying triangular TLP draft

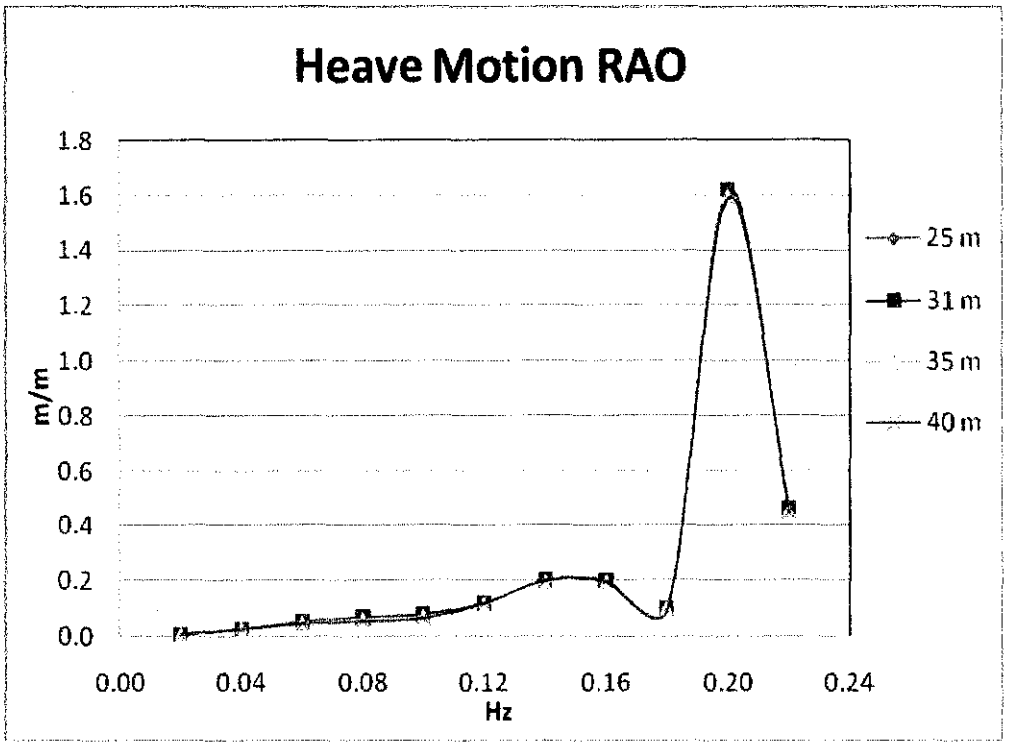

Figure 4.16 : Heave Motion RAO by varying triangular TLP draft

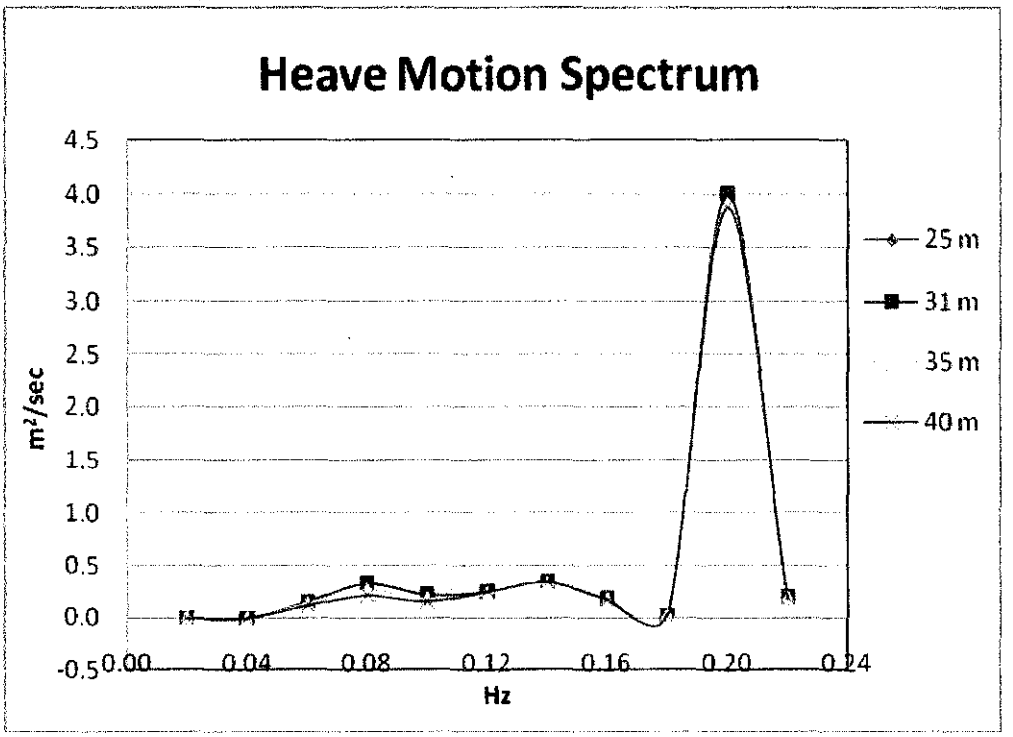

Figure 4.17 : Heave Motion Spectrum by varying triangular TLP draft

Table 4.3 : Maximum pitch response for different draft

Draft (m)	H_{max}, (m)	T (sec)	Pitch (degree)
25	24.4	12	-0.08
31	24.4	12	-0.10
35	24.4	12	-0.11
40	24.4	12	-0.09

4.3.4 Effect of Initial Tether Tension

Parametric study provides better understanding of the behavior of triangular TLP in open sea. Initial tether tension of in-place triangular TLP is one of them. In order to carry out this parametric study, sea state, stiffness, added mass and buoyancy of the structure were kept constant while only the total mass was changed. Initial tether tension being considered in this study are 165 500 kN, 135 500 kN, 105 500 kN, and 75 500 kN.

From figure 4.18, surge RAO is maximum when the initial tether tension of the triangular TLP is set at 105 500 kN. The respective frequency of wave is 0.02 Hz. Very high value of RAO at this frequency indicates that resonance is expected to occur in surge motion. Surge motion spectrum which represent energy density at different wave frequency shows its highest energy when the initial tether tension was set to be 165 000 kN. The respective wave frequency is 0.06 Hz.

Heave RAO is highest when the initial tether tension was set at 105 500 kN. The respective wave frequency is at 0.2 Hz. This wave frequency also contributed to highest energy density for heave motion spectrum for all set of initial tether tension. However, greatest energy density, 25 m^2/sec is resulted from 105 000 kN initial tether tension.

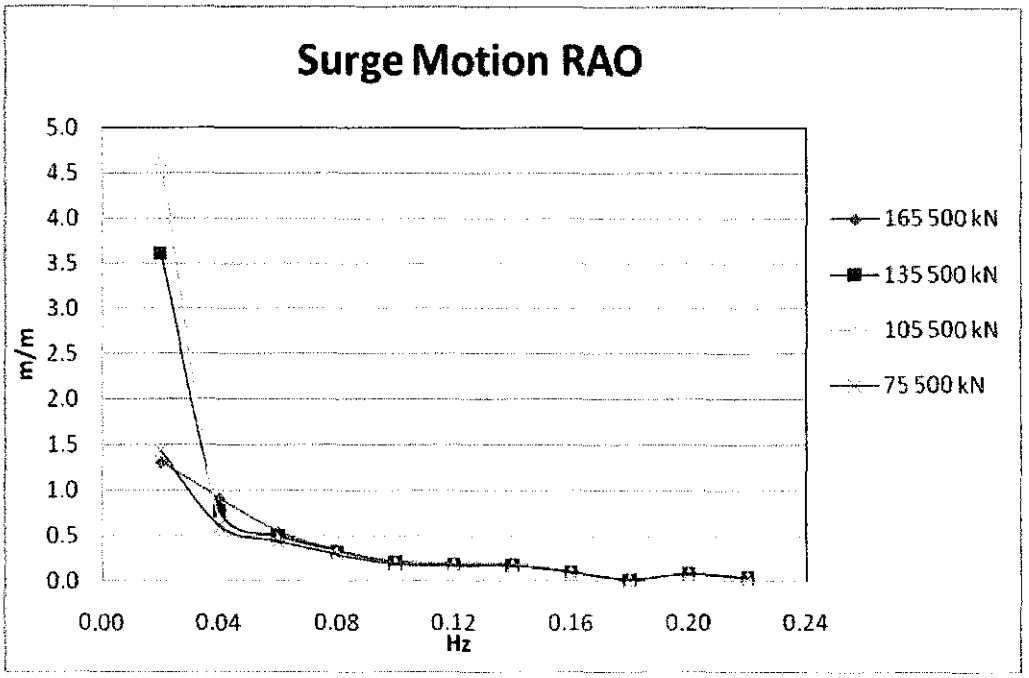

Figure 4.18 : Surge Motion RAO for different initial tether tension

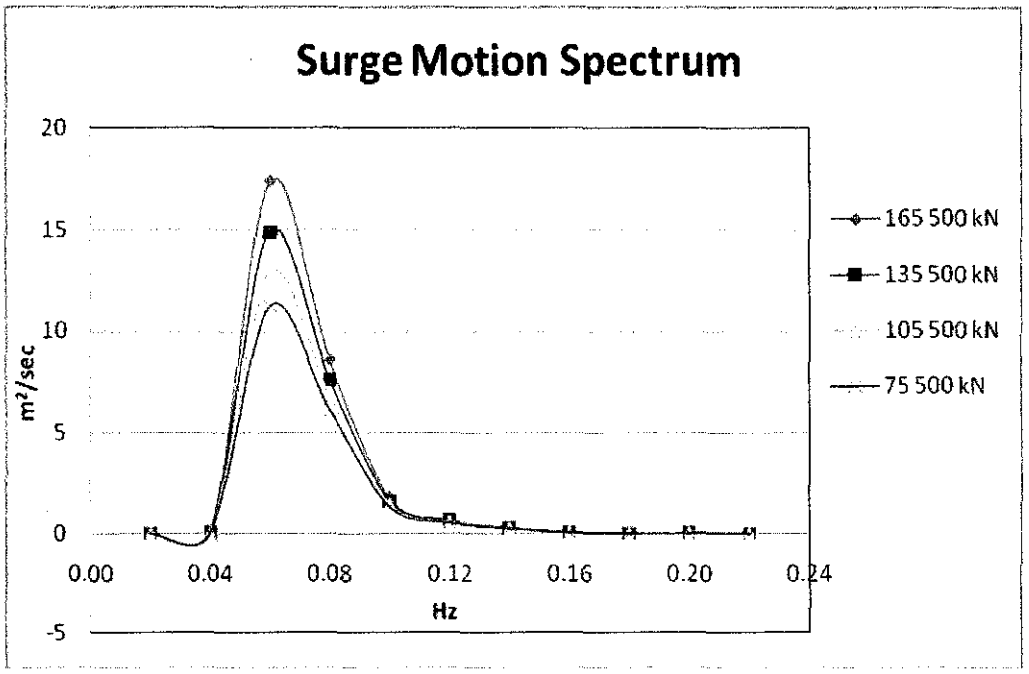

Figure 4.19 : Surge Motion Spectrum for different initial tether tension

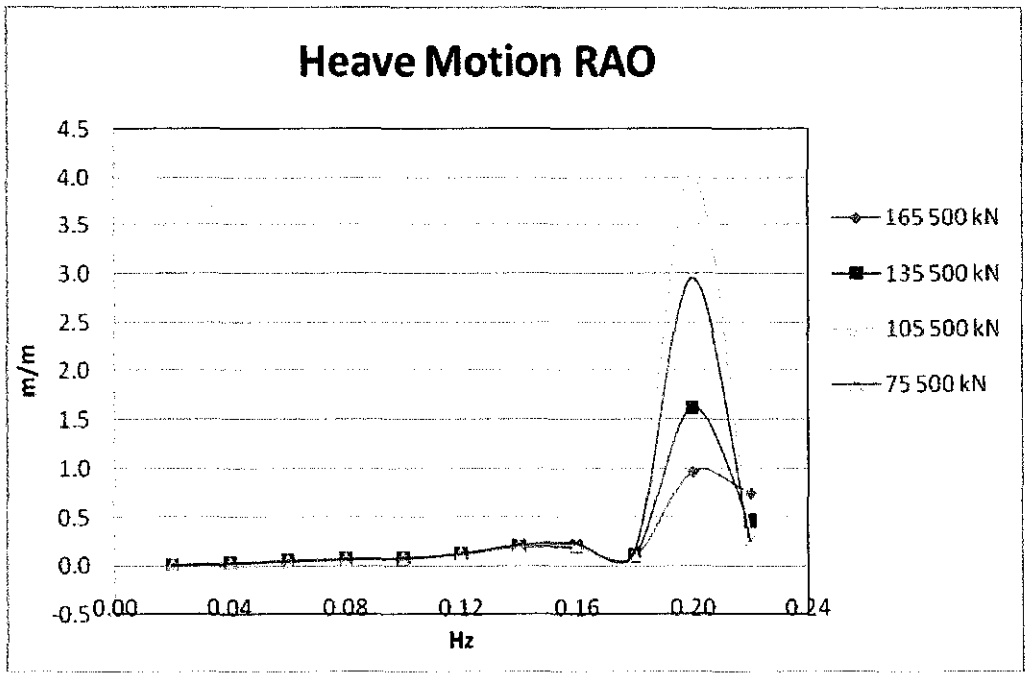

Figure 4.20 : Heave Motion RAO for different initial tether tension

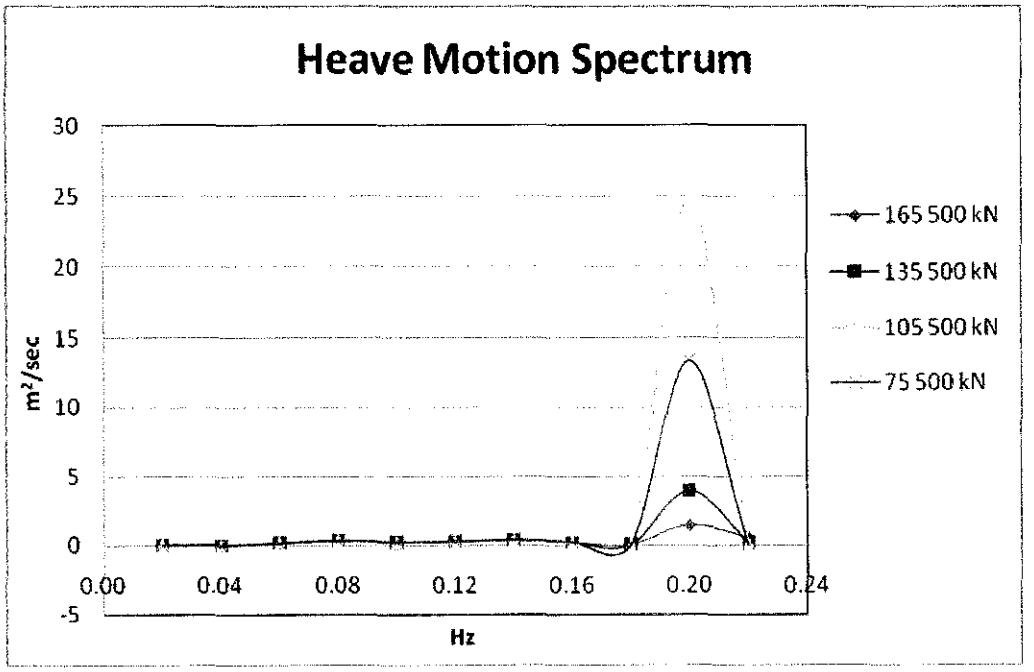

Figure 4.21 : Heave Motion Spectrum for different initial tether tension

Table 4.4 below shows the maximum pitch response of triangular TLP at different set of initial tether tension. The pitch response was analyzed for H_{max} resulted from H_s = 8 m. The TLP gives small pitch response for various initial tether tensions.

Table 4.4 : Maximum pitch response for various initial tether tension

Initial tether tension (kN)	H_{max}, (m)	T (sec)	Pitch (degree)
300 000	24.4	12	-0.10
330 000	24.4	12	-0.10
360 000	24.4	12	-0.09
390 000	24.4	12	-0.09

CHAPTER 5
CONCLUSIONS

Discussion on overall dynamic response of the triangular TLP has been made based on results obtained. The following conclusions were drawn from the frequency domain analysis :

- A dynamic analysis for random waves is carried out in the frequency domain by employing a simulation of sea state by P-M spectrum. The wave forces on the TLP hulls decreases as the water depth increases. Furthermore, when the wave parameter such as wave height, H or wave period T, and time, t changes, the wave forces will also change. From the result obtained it can be concluded that the wave forces acting upon the TLP hulls decreases exponentially as the water depth increases towards the TLP keel due to higher water particle velocity and acceleration near the water surface.

- Pierson-Moskowitz Spectrum representing the energy distribution of a wind generated sea state at different wave frequency gives a bell shaped curve. Simulation of wave surface profile from this spectrum by substituting the wave parameters into equation 2.11 produced produce a random wave profile.

- In general, the responses of the triangular TLP rely on the parameters involved in computing structure RAO. Surge and heave response of the structure are sensitive to wave heights and the triangular TLP properties as discussed in previous Chapter 4. Pitch only shows a small response to wave excitation upon the triangular TLP. This frequency domain analysis does not show an accurate result compared to time domain analysis. Nevertheless, its simplicity and reliable result makes it very applicable for TLP design all around the world.

REFERENCES

1. Adrezin R and Benoraya H, 1998 "Non-linear stochastic dynamics of tension leg platforms" Journal of Sound and Vibration 220, pg 27-65

2. Chandrasekaran.S and A.K. Jain, 2000 "Dynamic Behavior of Square and Triangular Offshore Tension Leg platforms Under Regular Wave Loads" Ocean Engineering 29(2002) pg 279-313.

3. Chakrabarti.S. 1987 "Hydrodynamics of Offsore Structures" Southhampton, UK, WIT Press.

4. Harald E. Krogstad & Øivind A. Arntsen 23 Feb 2003 http://folk.ntnu.no/oivarn/hercules_ntnu/LWTcourse/

5. Khan R.A., Siddiqui N.A, Naqvi S.Q.A, S. Ahmad S, 2004 "Reliability analysis of TLP tethers under impulsive loading" Reliability Engineering and System Safety 91, pg 73–83

6. Kim C.H, Lee C.H, Goo J.S, 2006 "A dynamic response analysis of tension leg platforms including hydrodynamic interaction in regular waves" Ocean Engineering 34, pg. 1680–1689

7. Kurian V.J., Idichandy V.G. and Ganapathy C., 1993 " Hydrodynamic Response of Tension-leg Platforms - A Model" Experimental Mechanics, pg 212-217

8. Lee H.H, Wang W.S, 2000 "On the dragged surge vibration of twin TLP systems with multi-interactions of wave and structures" Journal of Sound and Vibration 263, pg 743–774

9. Gadagi M, Benaroya H, 2004." Dynamic response of an axially loaded tendon of a tension leg platform" Rutgers University, USA

APPENDIX 1

Wave Force Calculation

WAVE PARAMETERS

Depth, d	300	m
Wave Period, T	4.545	sec
Wave Height, H	0.391	m
Water Density, ρ	1030	kg/m^3
Diameter Cylinder, D_{HULL}	16.39	m
Pontoon Diameter , $D_{PONTOON}$	12.58	m
Inertia Coefficient, C_m	2	
Drag Coefficient, C_d	1	
t	0	sec

a) Find wavelength, L

L_0 = 32.239 m

$L = L_o$ = 32.239 m

b) Wave Number, k

k = 0.195

c) Wave Frequency, ω

ω = 1.382

d) Wave Force

SECTION	FORCE (kN)			
	Fx	Fy	Fz	Resultant
Hull 1	813.048	0.000	0.000	813.048
Hull 2	813.048	0.000	0.000	813.048
Hull 3	-329.272	0.000	0.000	329.272
Pontoon 1	53.920	-11.059	0.000	55.042
Pontoon 2	-0.466	-2.308	0.806	2.489
Pontoon 3	-0.466	-2.308	-0.806	2.489
Total Wave Force	**1349.812**	**-15.675**	**0.000**	**1349.903**

e) Moment About COG = **-1712.87 kN.m**

Wave Force Calculation Sheet

Hull 1

Coordinate			s (m)	Length (m)	u (m/s)	v (m/s)	u' (m/s^2)	v' (m/s^2)	u_x (m/s)	u_y (m/s)	u_z (m/s)	u'_x (m/s^2)	u'_y (m/s^2)	u'_z (m/s^2)	w (m/s)	f_x kN	f_y kN	f_z kN	Total Force kN
X	Y	Z																	
-25.2173	0	43.68																	
-25.2173	-0.5	43.68	299.5	1.000	0.049	0.240	0.332	-0.068	0.049	0.000	0.000	0.332	0.000	0.000	0.049	144.326	0.000	0.000	**144.326**
-25.2173	-1	43.68																	
-25.2173	-1.5	43.68	298.5	1.000	0.041	0.198	0.273	-0.056	0.041	0.000	0.000	0.273	0.000	0.000	0.041	118.766	0.000	0.000	**118.766**
-25.2173	-2	43.68																	
-25.2173	-2.5	43.68	297.5	1.000	0.033	0.163	0.225	-0.046	0.033	0.000	0.000	0.225	0.000	0.000	0.033	97.733	0.000	0.000	**97.733**
-25.2173	-3	43.68																	
-25.2173	-3.5	43.68	296.5	1.000	0.027	0.134	0.185	-0.038	0.027	0.000	0.000	0.185	0.000	0.000	0.027	80.425	0.000	0.000	**80.425**
-25.2173	-4	43.68																	
-25.2173	-4.5	43.68	295.5	1.000	0.023	0.110	0.152	-0.031	0.023	0.000	0.000	0.152	0.000	0.000	0.023	66.183	0.000	0.000	**66.183**
-25.2173	-5	43.68																	
-25.2173	-5.5	43.68	294.5	1.000	0.019	0.091	0.125	-0.026	0.019	0.000	0.000	0.125	0.000	0.000	0.019	54.462	0.000	0.000	**54.462**
-25.2173	-6	43.68																	
-25.2173	-6.5	43.68	293.5	1.000	0.015	0.075	0.103	-0.021	0.015	0.000	0.000	0.103	0.000	0.000	0.015	44.818	0.000	0.000	**44.818**
-25.2173	-7	43.68																	
-25.2173	-7.5	43.68	292.5	1.000	0.013	0.061	0.085	-0.017	0.013	0.000	0.000	0.085	0.000	0.000	0.013	36.881	0.000	0.000	**36.881**
-25.2173	-8	43.68																	
-25.2173	-8	43.68																	
-25.2173	-8.5	43.68	291.5	1.000	0.010	0.051	0.070	-0.014	0.010	0.000	0.000	0.070	0.000	0.000	0.010	30.350	0.000	0.000	**30.350**
-25.2173	-9	43.68																	
-25.2173	-9.5	43.68	290.5	1.000	0.009	0.042	0.057	-0.012	0.009	0.000	0.000	0.057	0.000	0.000	0.009	24.976	0.000	0.000	**24.976**
-25.2173	-10	43.68																	
-25.2173	-10.5	43.68	289.5	1.000	0.007	0.034	0.047	-0.010	0.007	0.000	0.000	0.047	0.000	0.000	0.007	20.553	0.000	0.000	**20.553**
-25.2173	-11	43.68																	
-25.2173	-11.5	43.68	288.5	1.000	0.006	0.028	0.039	-0.008	0.006	0.000	0.000	0.039	0.000	0.000	0.006	16.913	0.000	0.000	**16.913**
-25.2173	-12	43.68																	
-25.2173	-12.5	43.68	287.5	1.000	0.005	0.023	0.032	-0.007	0.005	0.000	0.000	0.032	0.000	0.000	0.005	13.918	0.000	0.000	**13.918**
-25.2173	-13	43.68																	
-25.2173	-13.5	43.68	286.5	1.000	0.004	0.019	0.026	-0.005	0.004	0.000	0.000	0.026	0.000	0.000	0.004	11.454	0.000	0.000	**11.454**
-25.2173	-14	43.68																	
-25.2173	-14.5	43.68	285.5	1.000	0.003	0.016	0.022	-0.004	0.003	0.000	0.000	0.022	0.000	0.000	0.003	9.425	0.000	0.000	**9.425**
-25.2173	-15	43.68																	
-25.2173	-15.5	43.68	284.5	1.000	0.003	0.013	0.018	-0.004	0.003	0.000	0.000	0.018	0.000	0.000	0.003	7.756	0.000	0.000	**7.756**
-25.2173	-16	43.68																	

Hull 1

Coordinate			s (m)	Length (m)	u (m/s)	v (m/s)	u' (m/s^2)	v' (m/s^2)	u_x (m/s)	u_y (m/s)	u_z (m/s)	u'_x (m/s^2)	u'_y (m/s^2)	u'_z (m/s^2)	w (m/s)	f_x kN	f_y kN	f_z kN	Total Force kN
X	Y	Z																	
-25.2173	-16	43.68																	
-25.2173	-16.5	43.68	283.5	1.000	0.002	0.011	0.015	-0.003	0.002	0.000	0.000	0.015	0.000	0.000	0.002	6.383	0.000	0.000	**6.383**
-25.2173	-17	43.68																	
-25.2173	-17.5	43.68	282.5	1.000	0.002	0.009	0.012	-0.002	0.002	0.000	0.000	0.012	0.000	0.000	0.002	5.253	0.000	0.000	**5.253**
-25.2173	-18	43.68																	
-25.2173	-18.5	43.68	281.5	1.000	0.001	0.007	0.010	-0.002	0.001	0.000	0.000	0.010	0.000	0.000	0.001	4.322	0.000	0.000	**4.322**
-25.2173	-19	43.68																	
-25.2173	-19.5	43.68	280.5	1.000	0.001	0.006	0.008	-0.002	0.001	0.000	0.000	0.008	0.000	0.000	0.001	3.557	0.000	0.000	**3.557**
-25.2173	-20	43.68																	
-25.2173	-20.5	43.68	279.5	1.000	0.001	0.005	0.007	-0.001	0.001	0.000	0.000	0.007	0.000	0.000	0.001	2.927	0.000	0.000	**2.927**
-25.2173	-21	43.68																	
-25.2173	-21.5	43.68	278.5	1.000	0.001	0.004	0.006	-0.001	0.001	0.000	0.000	0.006	0.000	0.000	0.001	2.409	0.000	0.000	**2.409**
-25.2173	-22	43.68																	
-25.2173	-22.5	43.68	277.5	1.000	0.001	0.003	0.005	-0.001	0.001	0.000	0.000	0.005	0.000	0.000	0.001	1.982	0.000	0.000	**1.982**
-25.2173	-23	43.68																	
-25.2173	-23.5	43.68	276.5	1.000	0.001	0.003	0.004	-0.001	0.001	0.000	0.000	0.004	0.000	0.000	0.001	1.631	0.000	0.000	**1.631**
-25.2173	-24	43.68																	
-25.2173	-24	43.68																	
-25.2173	-24.5	43.68	275.5	1.000	0.000	0.002	0.003	-0.001	0.000	0.000	0.000	0.003	0.000	0.000	0.000	1.342	0.000	0.000	**1.342**
-25.2173	-25	43.68																	
-25.2173	-25.5	43.68	274.5	1.000	0.000	0.002	0.003	-0.001	0.000	0.000	0.000	0.003	0.000	0.000	0.000	1.105	0.000	0.000	**1.105**
-25.2173	-26	43.68																	
-25.2173	-26.5	43.68	273.5	1.000	0.000	0.002	0.002	0.000	0.000	0.000	0.000	0.002	0.000	0.000	0.000	0.909	0.000	0.000	**0.909**
-25.2173	-27	43.68																	
-25.2173	-27.5	43.68	272.5	1.000	0.000	0.001	0.002	0.000	0.000	0.000	0.000	0.002	0.000	0.000	0.000	0.748	0.000	0.000	**0.748**
-25.2173	-28	43.68																	
-25.2173	-28.5	43.68	271.5	1.000	0.000	0.001	0.001	0.000	0.000	0.000	0.000	0.001	0.000	0.000	0.000	0.616	0.000	0.000	**0.616**
-25.2173	-29	43.68																	
-25.2173	-29.5	43.68	270.5	1.000	0.000	0.001	0.001	0.000	0.000	0.000	0.000	0.001	0.000	0.000	0.000	0.507	0.000	0.000	**0.507**
-25.2173	-30	43.68																	
-25.2173	-30.5	43.68	269.5	1.000	0.000	0.001	0.001	0.000	0.000	0.000	0.000	0.001	0.000	0.000	0.000	0.417	0.000	0.000	**0.417**
-25.2173	-31	43.68																	
															TOTAL WAVE FORCE ON HULL 1		**813.048**	**0.000**	**0.000**	**813.048**

MOMENT CALCULATION ABOUT COG

HULL 1

F_X (kN)	Distance From COG, m	Moment, kN.m
144.33	3.03	437.31
118.77	2.03	241.09
97.73	1.03	100.66
80.43	0.03	2.41
66.18	-0.97	-64.20
54.46	-1.97	-107.29
44.82	-2.97	-133.11
36.88	-3.97	-146.42
30.35	-4.97	-150.84
24.98	-5.97	-149.10
20.55	-6.97	-143.25
16.91	-7.97	-134.80
13.92	-8.97	-124.85
11.45	-9.97	-114.19
9.43	-10.97	-103.40
7.76	-11.97	-92.84
6.38	-12.97	-82.79
5.25	-13.97	-73.38
4.32	-14.97	-64.71
3.56	-15.97	-56.81
2.93	-16.97	-49.67
2.41	-17.97	-43.29
1.98	-18.97	-37.60
1.63	-19.97	-32.58
1.34	-20.97	-28.15
1.10	-21.97	-24.27
0.91	-22.97	-20.88
0.75	-23.97	-17.93
0.62	-24.97	-15.37
0.51	-25.97	-13.16
0.42	-26.97	-11.24
	Total	-1254.64

HULL 2

F_X (kN)	Distance From COG, m	Moment, kN.m
144.33	3.03	437.31
118.77	2.03	241.09
97.73	1.03	100.66
80.43	0.03	2.41
66.18	-0.97	-64.20
54.46	-1.97	-107.29
44.82	-2.97	-133.11
36.88	-3.97	-146.42
30.35	-4.97	-150.84
24.98	-5.97	-149.10
20.55	-6.97	-143.25
16.91	-7.97	-134.80
13.92	-8.97	-124.85
11.45	-9.97	-114.19
9.43	-10.97	-103.40
7.76	-11.97	-92.84
6.38	-12.97	-82.79
5.25	-13.97	-73.38
4.32	-14.97	-64.71
3.56	-15.97	-56.81
2.93	-16.97	-49.67
2.41	-17.97	-43.29
1.98	-18.97	-37.60
1.63	-19.97	-32.58
1.34	-20.97	-28.15
1.10	-21.97	-24.27
0.91	-22.97	-20.88
0.75	-23.97	-17.93
0.62	-24.97	-15.37
0.51	-25.97	-13.16
0.42	-26.97	-11.24
	Total	-1254.64

HULL 3

F_X (kN)	Distance From COG, m	Moment, kN.m
58.64	3.03	177.68
48.19	2.03	97.83
39.62	1.03	40.80
32.57	0.03	0.98
26.79	-0.97	-25.98
22.03	-1.97	-43.40
18.12	-2.97	-53.81
14.90	-3.97	-59.17
12.26	-4.97	-60.94
10.09	-5.97	-60.22
8.30	-6.97	-57.85
6.83	-7.97	-54.42
5.62	-8.97	-50.40
4.62	-9.97	-46.09
3.80	-10.97	-41.73
3.13	-11.97	-37.47
2.58	-12.97	-33.41
2.12	-13.97	-29.61
1.74	-14.97	-26.11
1.44	-15.97	-22.92
1.18	-16.97	-20.04
0.97	-17.97	-17.46
0.80	-18.97	-15.17
0.66	-19.97	-13.14
0.54	-20.97	-11.36
0.45	-21.97	-9.79
0.37	-22.97	-8.42
0.30	-23.97	-7.23
0.25	-24.97	-6.20
0.20	-25.97	-5.31
0.17	-26.97	-4.54
	Total	-504.89

PONTOON 1

F_X (kN)	Distance From COG, m	Moment, kN.m
-7.70	-21.18	163.15
-7.70	-21.18	163.15
-7.70	-21.18	163.15
-7.70	-21.18	163.15
-7.70	-21.18	163.15
-7.70	-21.18	163.15
-7.70	-21.18	163.15
	Total	1142.02

F_Y (kN)	Distance From COG, m	Moment, kN.m
-1.58	25.22	-39.84
-1.58	25.22	-39.84
-1.58	25.22	-39.84
-1.58	25.22	-39.84
-1.58	25.22	-39.84
-1.58	25.22	-39.84
-1.58	25.22	-39.84
	Total	-278.87

PONTOON 2

F_X (kN)	Distance From COG, m	Moment, kN.m
0.88	-21.18	-18.72
1.61	-21.18	-34.17
-1.34	-21.18	28.38
-1.23	-21.18	26.14
1.69	-21.18	-35.78
0.76	-21.18	-16.03
-1.90	-21.18	40.31
	Total	-9.86

F_Y (kN)	Distance From COG, m	Moment, kN.m
7.02	13.73	96.41
-4.49	4.94	-22.19
-5.75	-3.85	22.14
6.12	-12.64	-77.33
4.02	-21.42	-86.17
-7.26	-30.21	219.25
-1.97	-39.00	76.84
	Total	228.94

PONTOON 3

F_X (kN)	Distance From COG, m	Moment, kN.m
0.88	-21.18	-18.72
1.61	-21.18	-34.17
-1.34	-21.18	28.38
-1.23	-21.18	26.14
1.69	-21.18	-35.78
0.76	-21.18	-16.03
-1.90	-21.18	40.31
	Total	-9.86

F_Y (kN)	Distance From COG, m	Moment, kN.m
7.02	13.73	96.41
-4.49	4.94	-22.19
-5.75	-3.85	22.14
6.12	-12.64	-77.33
4.02	-21.42	-86.17
-7.26	-30.21	219.25
-1.97	-39.00	76.84
	Total	228.94

Total moment about COG = -1712.87 kN.m

APPENDIX 2

Pierson-Moskowitz and Motion Spectra

SURGE MOTION SPECTRUM

$$S_x(f) = \left[\frac{\frac{F_I}{0.5H}}{[(K - m\omega^2)^2 + (C\omega)^2]^{\frac{1}{2}}}\right]^2 S(f)$$

H_s = 8 m

a = 0.0081

ω_o = 0.4442 rad/sec

f_o = 0.0707 Hz

K_{SURGE} = 1511152.416 N/m

m_{SURGE} = 82050156.7 kg

C = 222702

f	T	ω	S(f)	Area S(f)Δf	H(f)	F_I	$L=L_o$	RAO_{SURGE}	$S_{SURGE}(f)$	Response (m)
0.02	50.000	0.126	0.000	0.000	0.000	0.000	3901.683	3.615	0.000	0.000
0.04	25.000	0.251	0.025	0.000	0.063	90.405	975.421	0.786	0.015	0.025
0.06	16.667	0.377	57.715	1.154	3.039	7822.602	433.520	0.507	14.848	0.771
0.08	12.500	0.503	71.140	1.423	3.374	10609.933	243.855	0.327	7.618	0.552
0.10	10.000	0.628	36.568	0.731	2.419	7833.163	156.067	0.210	1.609	0.254
0.12	8.333	0.754	17.275	0.346	1.663	7181.404	108.380	0.191	0.633	0.159
0.14	7.143	0.880	8.566	0.171	1.171	6804.522	79.626	0.188	0.301	0.110
0.16	6.250	1.005	4.544	0.091	0.853	3705.959	60.964	0.107	0.052	0.046
0.18	5.556	1.131	2.567	0.051	0.641	845.370	48.169	0.026	0.002	0.008
0.20	5.000	1.257	1.532	0.031	0.495	2764.879	39.017	0.087	0.012	0.022
0.22	4.545	1.382	0.957	0.019	0.391	1352.721	32.245	0.045	0.002	0.009

H_s = 8.018 m

H_{rms} = 5.669 m

HEAVE MOTION SPECTRUM

$$S_x(f) = \left[\frac{\frac{F_I}{0.5H}}{[(K - m\omega^2)^2 + (C\omega)^2]^{\frac{1}{2}}}\right]^2 S(f)$$

H_s	=	8 m	K_{HEAVE}	=	108392903.6 N/m
σ	=	0.0081	m_{HEAVE}	=	64472021.27 kg
ω_o	=	0.4442 rad/sec	C	=	1671922
f_o	=	0.0707 Hz			

f	T	ω	S(f)	Area S(f)Δf	H(f)	F_I	$L=L_o$	RAO_{HEAVE}	$S_{HEAVE}(f)$	Response (m)
0.02	50.000	0.126	0.000	0.000	0.000	0.000	3901.683	0.007	0.000	0.000
0.04	25.000	0.251	0.025	0.000	0.063	90.405	975.421	0.028	0.000	0.001
0.06	16.667	0.377	57.715	1.154	3.039	7822.602	433.520	0.052	0.155	0.079
0.08	12.500	0.503	71.140	1.423	3.374	10609.933	243.855	0.068	0.332	0.115
0.10	10.000	0.628	36.568	0.731	2.419	7833.163	156.067	0.078	0.223	0.094
0.12	8.333	0.754	17.275	0.346	1.663	7181.404	108.380	0.120	0.250	0.100
0.14	7.143	0.880	8.566	0.171	1.171	6804.522	79.626	0.199	0.338	0.116
0.16	6.250	1.005	4.544	0.091	0.853	3705.959	60.964	0.201	0.183	0.086
0.18	5.556	1.131	2.567	0.051	0.641	845.370	48.169	0.101	0.026	0.033
0.20	5.000	1.257	1.532	0.031	0.495	2764.879	39.017	1.617	4.003	0.400
0.22	4.545	1.382	0.957	0.019	0.391	1352.721	32.245	0.462	0.204	0.090

H_s	=	8.018 m
H_{rms}	=	5.669 m

PITCH MOTION SPECTRUM

$$S_x(f) = \left[\frac{\frac{F_I}{0.5H}}{[(K - m\omega^2)^2 + (C\omega)^2]^{\frac{1}{2}}}\right]^2 S(f)$$

H_s	=	8 m		K_{PITCH}	=	6.752E+11	N.m/rad
α	=	0.0081		m_{PITCH}	=	7.943E+10	kg
ω_o	=	0.4442	rad/sec	C	=	4.632E+09	
f_o	=	0.0707	Hz				

f	T	ω	S(f)	Area S(f)Δf	H(f)	F_I	$L=L_o$	RAO_{PITCH}	$S_{PITCH}(f)$	Response (degree)
0.02	50.000	0.126	0.000	0.000	0.000	0.000	3901.683	0.000	0.000	0.0000
0.04	25.000	0.251	0.025	0.000	0.063	-274.462	975.421	0.000	0.000	0.0000
0.06	16.667	0.377	57.715	1.154	3.039	-52483.573	433.520	0.000	0.000	-0.0045
0.08	12.500	0.503	71.140	1.423	3.374	-138963.019	243.855	0.000	0.000	-0.0122
0.10	10.000	0.628	36.568	0.731	2.419	-151975.502	156.067	0.000	0.000	-0.0135
0.12	8.333	0.754	17.275	0.346	1.663	-104757.730	108.380	0.000	0.000	-0.0095
0.14	7.143	0.880	8.566	0.171	1.171	-65688.377	79.626	0.000	0.000	-0.0061
0.16	6.250	1.005	4.544	0.091	0.853	-21583.632	60.964	0.000	0.000	-0.0021
0.18	5.556	1.131	2.567	0.051	0.641	2709.388	48.169	0.000	0.000	0.0003
0.20	5.000	1.257	1.532	0.031	0.495	-1666.718	39.017	0.000	0.000	-0.0002
0.22	4.545	1.382	0.957	0.019	0.391	-1711.167	32.245	0.000	0.000	-0.0002

H_s	=	8.018	m
H_{rms}	=	5.669	m

RANDOM WAVE PROFILE

$$\eta(x,t) = \sum_{n=1}^{N} \frac{H(n)}{2} \cos\left[k(n)x - 2\pi f(n)t + \varepsilon(n)\right]$$

H_s = 8 m

α = 0.0081

ω_o = 0.4442 rad/sec

f_o = 0.0707 Hz

f	S(f)	Area S(f)Δf	H(n)	L(n)=L_o	k(n)	x	R_N	ε(n)
0.06	57.715	3.463	5.263	433.520	0.014	-25.217	0.715	4.493
0.08	71.140	1.423	3.374	243.855	0.026	-25.217	0.004	0.022
0.1	36.568	0.731	2.419	156.067	0.040	-25.217	0.746	4.686
0.12	17.275	0.346	1.663	108.380	0.058	-25.217	0.053	0.334
0.14	8.566	0.171	1.171	79.626	0.079	-25.217	0.226	1.420
0.16	4.544	0.091	0.853	60.964	0.103	-25.217	0.707	4.442
0.18	2.567	0.051	0.641	48.169	0.130	-25.217	0.632	3.970
0.2	1.532	0.031	0.495	39.017	0.161	-25.217	0.906	5.690
0.22	0.957	0.019	0.391	32.245	0.195	-25.217	0.111	0.698
0.24	0.622	0.012	0.315	27.095	0.232	-25.217	0.389	2.444

f	η(x,t) at time, t										
	1	2	3	4	5	6	7	8	9	10	11
0.06	-2.280	-1.636	-0.763	0.218	1.168	1.954	2.466	2.631	2.427	1.882	1.073
0.08	1.622	1.198	0.478	-0.360	-1.110	-1.584	-1.667	-1.338	-0.677	0.151	0.942
0.10	-1.104	-1.183	-0.811	-0.128	0.603	1.104	1.183	0.811	0.128	-0.603	-1.104
0.12	-0.626	-0.082	0.506	0.820	0.690	0.185	-0.420	-0.797	-0.742	-0.285	0.327
0.14	-0.410	-0.583	-0.333	0.158	0.535	0.524	0.133	-0.355	-0.585	-0.391	0.086
0.16	0.266	-0.139	-0.415	-0.305	0.088	0.399	0.340	-0.035	-0.377	-0.370	-0.019
0.18	-0.293	-0.243	0.086	0.316	0.183	-0.160	-0.319	-0.112	0.224	0.303	0.034
0.20	-0.247	-0.059	0.210	0.189	-0.093	-0.247	-0.059	0.210	0.189	-0.093	-0.247
0.22	-0.050	-0.195	-0.023	0.187	0.093	-0.152	-0.150	0.096	0.186	-0.026	-0.195
0.24	0.152	0.050	-0.146	-0.068	0.138	0.085	-0.127	-0.101	0.114	0.116	-0.100
$\Sigma\eta$(x,t)	-2.970	-2.874	-1.210	1.026	2.295	2.109	1.380	1.010	0.886	0.683	0.796

f	η(x,t) at time, t										
	12	13	14	15	16	17	18	19	20	21	22
0.06	0.113	-0.863	-1.718	-2.331	-2.617	-2.535	-2.098	-1.365	-0.441	0.545	1.454
0.08	1.499	1.686	1.456	0.865	0.061	-0.759	-1.391	-1.679	-1.551	-1.040	-0.272
0.10	-1.183	-0.811	-0.128	0.603	1.104	1.183	0.811	0.128	-0.603	-1.104	-1.183
0.12	0.761	0.783	0.381	-0.228	-0.714	-0.812	-0.470	0.126	0.654	0.828	0.553
0.14	0.501	0.553	0.203	-0.293	-0.577	-0.443	0.013	0.459	0.572	0.270	-0.228
0.16	0.349	0.393	0.072	-0.316	-0.411	-0.124	0.278	0.422	0.174	-0.235	-0.426
0.18	-0.274	-0.267	0.046	0.307	0.215	-0.124	-0.320	-0.149	0.193	0.314	0.074
0.20	-0.059	0.210	0.189	-0.093	-0.247	-0.059	0.210	0.189	-0.093	-0.247	-0.059
0.22	-0.047	0.178	0.114	-0.135	-0.164	0.073	0.192	-0.002	-0.192	-0.071	0.166
0.24	-0.128	0.084	0.139	-0.066	-0.147	0.048	0.153	-0.028	-0.157	0.009	0.158
$\Sigma\eta$(x,t)	1.532	1.946	0.754	-1.688	-3.497	-3.552	-2.622	-1.898	-1.443	-0.731	0.236

f	η(x,t) at time, t										
	23	24	25	26	27	28	29	30	31	32	33
0.06	2.160	2.562	2.604	2.280	1.636	0.763	-0.218	-1.168	-1.954	-2.466	-2.631
0.08	0.564	1.260	1.645	1.622	1.198	0.478	-0.360	-1.110	-1.584	-1.667	-1.338
0.10	-0.811	-0.128	0.603	1.104	1.183	0.811	0.128	-0.603	-1.104	-1.183	-0.811
0.12	-0.022	-0.585	-0.831	-0.626	-0.082	0.506	0.820	0.690	0.185	-0.420	-0.797
0.14	-0.561	-0.487	-0.060	0.410	0.583	0.333	-0.158	-0.535	-0.524	-0.133	0.355
0.16	-0.222	0.189	0.424	0.266	-0.139	-0.415	-0.305	0.088	0.399	0.340	-0.035
0.18	-0.251	-0.287	0.006	0.293	0.243	-0.086	-0.316	-0.183	0.160	0.319	0.112
0.20	0.210	0.189	-0.093	-0.247	-0.059	0.210	0.189	-0.093	-0.247	-0.059	0.210
0.22	0.133	-0.116	-0.176	0.050	0.195	0.023	-0.187	-0.093	0.152	0.150	-0.096
0.24	0.011	-0.156	-0.031	0.152	0.050	-0.146	-0.068	0.138	0.085	-0.127	-0.101
$\Sigma\eta$(x,t)	1.211	2.439	4.090	5.305	4.809	2.478	-0.475	-2.870	-4.432	-5.246	-5.131

APPENDIX 3

Stiffness

(Surge, Heave and Pitch)

Stiffness in Surge

Total Weight	**330000**	kN
Initial Tether Tension, T_0	**135500**	kN/m
Tether Length	**269**	m
Stiffness of Tethers, K_{TETHER}	**34000**	kN/m
No. of Tethers	**3**	

Buoyancy Force, Fb 465500 kN

K_{SURGE} = No. of tethers X T_0 / L_{TETHER}

= 3 X 135500 / 269

= **1511.1524** **kN/m**

Stiffness in Heave

Total Weight	330000	kN
Initial Tether Tension, T_0	135500	kN/m
Tether Length	269	m
Stiffness of Tethers, K_{TETHER}	34000	kN/m
No. of Tethers	3	

Buoyancy Force, Fb 465500 kN

K_{HEAVE} = (No. of tethers X K_{TETHER}) + ($3\pi D^2_{HULL}$ / 4 X 1030 X 9.806 X 10^{-3})

= 102000 + 6392.9036

= **108392.9** **kN/m**

Stiffness in Pitch

T_{PITCH} 2.155 sec

m_{PITCH} 7.943E+10 kg

$$\omega_{PITCH} = \frac{2\pi}{T_{PITCH}}$$

$$= 2.916 \text{ rad/sec}$$

$$K_{PITCH} = \omega_{PITCH}^2 \times m_{PITCH}$$

$$= 8.501 \times 7.943E+10$$

$$= 6.752E+11$$

APPENDIX 4

Total Mass

(Surge, Heave and Pitch)

Mass of Surge

Mass of Surge, m_{SURGE} = Mass, m + Added Mass, m_{as}

Weight of Structure = 330000 kN

Mass of Structure, m = **33652866 kg**

Added mass, m_{as} = $[V_{HULLS} + V_{PONTOON1} + 2(V_{PONTOON}\cos 60 + \pi D^3_{PONTOON}/12 \times \cos 30)] \times 1030$

= (19621.434 + 8821.1655 + 18545.062) X 1030

= 46987.661 X 1030

= **48397291 kg**

m_{SURGE} = Mass of Structure + Added Mass

= 33652866 + 48397291

= **82050157 kg**

Mass of Heave

Mass of Heave, m_{HEAVE} = Mass, m + Added Mass, m_{ah}

Weight of Structure = 330000 kN
Mass of Structure, m = **33652866 kg**

Added mass, m_{ah} = $[(3 \times \pi D^3_{HULL}/12 + 3 \times \pi D^2_{PONTOON} / 4 \times L_{PONTOON}) \times 1030$

= (3458.014 + 26463.496) X 1030

= 29921.51 X 1030

= **30819156 kg**

m_{HEAVE} = Mass of Structure + Added Mass

= 33652866 + 30819156

= **64472021 kg**

Mass of Pitch

Mass of Pitch, m_{PITCH} = $m_{HEAVE} \times r_z^2$

Weight of Structure	=	**330000** kN
Mass of Structure, m	=	**33652865.59 kg**
rx	=	**35.1 m**
ry	=	**42.4 m**
rz	=	**35.1 m**

Added mass, m_{ah} = $[(3 \times \pi D^3_{HULL}/12 + 3 \times \pi D^2_{PONTOON} / 4 \times L_{PONTOON}) \times 1030$

= (3458.013959 + 26463.496) X 1030

= 29921.51037 X 1030

= 30819155.68 kg

m_{HEAVE} = Mass of Structure + Added Mass

= 33652865.59 + 30819156

= 64472021.27 kg

m_{PITCH} = m_{HEAVE} x r_z^2

= 64472021.27 x 1232.01

= **7.943E+10 kg**